FUNCTIONAL INVESTIGATION OF AN RNA BINDING PROTEIN WITH METHYL-TRANSFERASE DOMAIN

Ph.D. Thesis

by

Izzet Enünlü

Supervisor

Prof. Dr. Boros Imre

Institute of Biochemistry

Laboratory of Eukaryotic Transcription Regulation

Biological Research Center

Hungarian Academy of Sciences

Szeged

2003

TABLE OF CONTENTS

List of Abbreviations

ARM	arginine rich motif
Bp	base pair(s)
BSA	bovine serum albumin
CBP	cAMP-responsive transcription factor binding protein
DAPI	4', 6-diamidino-2-phenylindole HCl
DMEM	Dulbecco's modified Eagle's medium
DMSO	dimethyl sulfoxide
DsRBD	double stranded RNA binding domain
DTL	*Drosophila* Tat like
DTT	dithiothreitol
EED	embryonic ectoderm development
ESC	extra sex combs
EST	expressed sequence tags
EDTA	ethylenediamine tetraacetic acid
FCS	fetal calf serum
FITC	fluorescein isothiocyanate
HEPES	4-(2-hydroxyethyl)-1-piperazineethanesulfonic acid
HIV	human immunodeficiency virus
HnRNP	heteregeneous nuclear ribonucleoprotein
KH	K-homology domain
LTR	long terminal repeat
MAP	microtubule-associated proteins
mRNA	messenger ribonucleic acid
Nm	2'-O-methylated nucleosides
ONPG	o-nitrophenyl β-D-galactopyranoside
ORF	open reading frame

PAGE	polyacrylamide gel electrophoresis
PBS	phosphate buffered saline
PEG	polyethylene glycol
PIMT	PRIP-interacting protein with methyltransferase domain
PMSF	phenylmethylsulfonyl fluoride
PRIP	peroxisome proliferator-activated receptor-interacting protein
Ψ	pseudo
PTB	polypyrimidine-tract-binding protein
RNA	ribonucleic acid
RNP	ribonucleoprotein
rRNA	ribosomal ribonucleic acid
RRM	RNA recognition motif
SDS	sodium dodecyl sulfate
siRNA	small interfering ribonucleic acid
snRNA	small nuclear ribonucleic acid
snoRNA	small nucleolar ribonucleic acid
snRNP	small nuclear ribonucleoprotein
TAK	Tat-associated kinase
Tat	Transactivating regulatory protein
TAR	trans- activation-responsive RNA
TRITC	tetramethyl rhodamine isothiocyanate
tRNA	transfer ribonucleic acid

1. INTRODUCTION

RNA-protein interactions direct a diverse variety of cellular processes, which range from transcriptional regulation to targeted translation of proteins. Hence, to discover new proteins with a specific affinity to RNA molecules and find out their specific function will expand our understanding on a wide range of cellular functions. Following this statement, a screen was developed to search *Drosophila* proteome for RNA binding proteins and an unknown protein with RNA binding property was retrieved (Udvardy et al.). In this work we aimed to characterize this new *Drosophila* protein and its mammalian homologue.

The retrieved protein had well conserved homologues in different species and is represented with many ESTs (expressed sequence tags) in databases suggesting an important role in cellular function. In the beginning of our work none of the homologues had an identified function. However during our investigation, other research groups revealed certain aspects of the functional properties of this new class of proteins.

In the light of these new data, a retrospect evaluation of the work might lead an outside observer to the confusion in understanding our strategy. However, I believe that if the thesis developed on the path that we followed it would be easier to understand our aims and results. This is why current knowledge about this new class of protein that is found in the literature will be introduced in the discussion section.

1.1. Theoretical Background

Although once RNA was thought to be a passive genetic blueprint, now it is known as a key player in a wide variety of cellular processes. An RNA molecule conforms into double helices of base-complementary strands with a combination of deviations from plain helix such as hairpins, stem-loops, symmetrical or asymmetric interior loops, bulge loops, purine-purine

mispairs, GU or wobble pairs and pseudoknots (1,2). The combination of helical stems separated with the above non-helical motifs, provide RNA molecules the ability to form intricate three-dimensional architectures comparable to the complexity of protein folds. RNA binding proteins target these three dimensional arrangements for recognition. As a result, a great diversity in RNA and RNA binding structural motifs is observed.

1.1.1. RNA Binding Proteins

RNA-binding proteins have a modular structure and contain RNA binding domains of 70-150 amino acids that mediate RNA recognition. There are three major classes of eukaryotic RNA-binding domains:

1. The RNA recognition motif (RRM):

   The RRM or ribonucleoprotein (RNP) domain is approximately 100 amino acids long and found in a variety of RNA binding proteins, including various hnRNP proteins, proteins implicated in regulation of alternative splicing, and protein components of small nuclear ribonucleoproteins (snRNPs). This motif also appears in a few single stranded DNA binding proteins. Almost all RRM domains studied have a four-stranded β sheet packed against two α helices. One exception to this structure is the polypyrimidine-tract-binding protein (PTB), which contains an extra fifth strand in the β sheet (3).

2. K-homology domain (KH):

   This domain was first identified in human hnRNP K protein. It is an evolutionarily conserved sequence of around 70 amino acids that is present in a wide variety of quite diverse nucleic acid-binding proteins. Like many other RNA-binding motifs, KH motifs are found in one or multiple copies. KH domains have a similar αβ structure like RRM domains. This domain

has an invariant Gly-X-X-Gly segment (where X represents lysine, arginine or glycine), and another, more variable region (4).

3. Double stranded RNA binding domain (dsRBD):

   dsRBD is about 65 amino acids long and can bind dsRNA specifically. dsRBD proteins are mainly involved in posttranscriptional gene regulation, for example by preventing the expression of proteins or by mediating localization of RNAs. This domain is also found in RNA editing proteins. dsRBD binds dsRNA without sequence specificity. However, multiple dsRBDs may be able to act in combination to recognize the secondary structure of specific RNAs (5).

In addition to these RNA binding domains, there are many other less common motifs and domains to recognize RNAs. Some of them are:

- Zinc fingers:

  Zinc fingers are modules of approximately 30 amino acids containing an α helix and a β sheet coordinated by a zinc ion, and are often found in tandem repeats in proteins. Most zinc fingers bind to specific DNA sequences, recognizing approximately three base pairs per finger. However, some fingers also bind RNA (6).

- Arginine rich motif (ARM):

  The ARM is typically less than 20 amino acids long and binds RNA in α-helical, β-hairpin and extended conformations, depending on the peptide sequence and RNA site. The difference, which separates the arginin-rich motif (ARM) from previous examples, is that it requires an RNA binding to adopt a stable structure (7).

Formation of almost every RNA-protein complex involves conformational changes in the protein, the RNA, or both. RNA-protein interaction stabilizes both components into a

metabolically active structure (8). RNA binding motifs are also combined with other conserved domains, such as protein-interaction domains and catalytic domains.

RNA-binding proteins themselves or together with their RNA component, (ribonucleoprotein complexes (RNPs) play a central role in a wide range of functions of living cells such as transcriptional regulation (9,10), RNA editing (11), telomere maintenance (12), splicing (13), nucleo-cytoplasmic transport and localization of mRNA (14-16), translation (17), and stability (18).

Since to cover all these functional properties even at an introductory level, is both beyond the capacity and the scopes of this thesis, I am going to describe only some of the subjects related to my work.

1.1.2. RNA Editing

Several phenomena are included under the title RNA editing; these include nucleotide modifications (19-21) and post-transcriptional insertions and/or deletions (22,23), sometimes involving the participation of a guide RNA. The phenomenon of RNA-guided nucleotide modification is the conversion of a nucleotide in a precursor RNA to another form by an RNA-protein complex. The ribonucleoproteins (RNPs) that mediate these reactions include a small nucleolar RNA (snoRNA) that provides the guide function through base pairing with the substrate and a set of proteins, one of which catalyzes the modification reaction. Two common modifications exist, formation of 2'-O-methylated (Nm) nucleosides and conversion of uridine to pseudo (Ψ) uridine. These modifications are mediated by two large, heterogeneous populations of RNPs that are modification type-specific and site-specific (21).

The maturation process of rRNAs and small stable RNAs such as splicing snRNAs, tRNAs, and snoRNAs involve both 2'-O-methylations and pseudouridylations. Blocking of these

modifications in yeast rRNA has strong negative effects on growth rate (19). The changes in RNA structure caused by modification are believed to affect many events in rRNA folding, rRNP assembly, or ribosome activity as well as trafficking and half-life. The same reasoning applies to modification of the small RNAs.

The 2'-O-methylation guide snoRNAs contain sequence elements called boxes C and D which define the C/D family of snoRNAs. The canonical C/D boxes are required for snoRNA stability and proper end formation. Four proteins that are common components of box C/D snoRNPs have been characterized in yeast (and humans) are: Snu13p (15.5 kDa), Nop56p (hNop56p), Nop58p (hNop58p), and Nop1p (fibrillarin) (19). All of these proteins are essential for the function of the particle. Nop1p, Snu13p, and Nop58p are required for snoRNA stability and accumulation. Nop1p (fibrillarin) is generally accepted to be the 2'-O-methyltransferase (19).

The Ψ guide snoRNAs have hairpin-hinge-hairpin-tail structure referred to as boxes H and ACA and are members of a larger family of H/ACA snoRNAs. Like the C/D elements, the H and ACA boxes and neighboring duplexes are required for processing of snoRNA precursors, protein binding, and localization. The four core proteins of the H/ACA snoRNPs differ from those in the C/D snoRNPs. These are in yeast (and human) included: Cbf5p (dyskerin), Gar1p (hGar1p), Nhp2p (hNhp2p), and Nop10p (hNop10p). Cbf5p is accepted to be the pseudouridine synthase (19).

Most H/ACA snoRNAs are guide RNAs. However, as with the C/D snoRNA family, a few participate in rRNA processing, and one, telomerase RNA (from mammals but not yeast), guides telomere formation (24).

1.1.3. Spliceosomes

Splicing of precursor messenger RNAs is an important and ubiquitous type of gene regulation in metazoans. Splicing joins the coding sequences called exons by removing the intervening noncoding sequences, introns, from primary transcripts (25).

The intron is cleaved from the exons at the 5′ and 3′ ends, called the splice sites. These sequence elements must be recognized by the spliceosome, a multi-unit complex of proteins and RNA. The RNA components are small nuclear RNAs, U1, U2, U4, U5 and U6, assembled into ribonucleoprotein particles (snRNPs) (26).

SnRNPs assemble onto the intron substrate in a step-wise fashion, directed by interactions of snRNAs with intron consensus sequences. Correct selection of the splice sites is vital for gene expression, and regulating the use of different possible splice sites is fundamental to alternative splicing. As a result regulated splicing events are also mediated in part or entirely by elements of the splicing apparatus (27,28).

1.1.4. Transcriptional Trans-activation and TAT

Less frequently RNAs are involved directly in transcription modulation as well. One example of this is TAT, the transcriptional transactivation protein of HIV. The Tat-TAR ribonucleoprotein (RNP) is the essential switch that controls transcription from the HIV-1 long terminal repeats (LTR). The transactivator (Tat) binds to the trans-acting response element (TAR) found at the 5' end of viral transcripts, as a hairpin formation (29). The minimum Tat sequence that can mediate specific TAR binding *in vitro* has been mapped to a basic domain, comprising mostly Arg and Lys residues (30). TAR is absolutely required for TAT mediated transcriptional activity. After binding to TAR RNA, Tat stimulates a specific protein kinase called TAK (Tat-associated kinase) (9). This results in hyperphosphorylation of the large subunit of the RNA polymerase II carboxyl- terminal domain (9).

Tat-induced transcriptional activation of the LTR promoter is followed by the recruitment of the transcriptional coactivators p300 and cAMP-responsive transcription factor binding protein (CBP) (31). These large proteins bridge the basal transcription machinery with specific transcriptional activators for transcriptional initiation. P300/CBP are histone acetyl-transferases capable of modulating the interaction of nucleosomes with DNA and with chromatin remodeling complexes (32). Besides histones, Tat itself is a substrate for the enzymatic activity of p300/CBP suggesting a regulatory role of acetylation on the protein itself (33).

Recently, it was found that Tat binds tubulin/microtubules through a four-amino-acid subdomain of its conserved core region (34). This interaction alters the microtubule dynamics and activates a mitochondria-dependent apoptotic pathway.

Tat–tubulin interaction domain differ from those present in the tubulin-binding domains of general microtubule-associated proteins (MAPs), which typically contain positively charged residues (34). The arginine-rich domain of Tat which is adjacent to the tubulin-binding subdomain might provide the positive charge to neutralize the negatively charged tubulin C-termini in order to promote microtubule assembly (34).

1.2. Aims of the thesis

In this work we aimed to characterize a newly identified protein with RNA binding ability. A screen was designed to detect RNA binding proteins in *Drosophila* proteome by testing their affinity against the TAR RNA of Human Immunodeficiency Virus (Udvardy et al.). A previously unidentified protein was retrieved from this screen and named Drosophila TAT Like (DTL). Surprisingly, proteins related to DTL can be identified in a wide range of organisms. From yeast to human they share well-conserved boxes of amino acids characteristic for RNA methyltransferases. The presence of large number of ESTs in databases indicates that the genes encoding these proteins are intensively expressed as well.

The general aims of the study were:

- To identify homologues of DTL by performing similarity searches against the known sequences found in databases,
- By using the data obtained from similarity searches:
  1. to determine conserved regions which will point out functional regions or motifs of DTL related proteins,
  2. to find EST (expressed sequence tags) sequences belonging to mammalian homologues of DTL, to work in parallel with *Drosophila* sequences,
- To test whether the conserved motifs or domains that are found are functional,
- To characterize the expression pattern and the possible isoforms of DTL and its mammalian homologues. For this purpose we raised specific polyclonal antibodies, and we analyzed protein samples from different tissues and compartments of the cell, by Western blotting and immunolocalization,
- To find partner proteins of DTL and its mammalian homologues and determine the nature of interacting structures, by using *in vitro* or *in vivo* techniques like yeast two hybrid screen and immunolocalization,
- To attribute a functional property for the DTL related proteins in cellular events, by siRNA knock down in established cell lines.

2. MATERIALS AND METHODS

2.1. Cell culture techniques

Mammalian HeLa cell line was cultured in Dulbecco's modified Eagle's medium (DMEM) containing 5% fetal calf serum (FCS; Gibco/BRL, Gaithesburg, MD/USA) in incubator at 37°C with 5% CO_2. Drosophila Schneider S2 cell line was cultured in Schneider's insect medium containing 10% fetal calf serum at 22°C. Three times per week cultures were expanded to maintain logarithmic growth. For immunolocalization experiments, cells were grown adherent on cover slips.

For transfection, cells were plated in 6 well plates at a density of 1.5-2.0 x 10^5 cells per well. 24 hours after seeding, the cells were transfected with Xgene (Fermentas) according to manufacturer's instructions.

For cell cycle studies, cells were seeded at a density of 1.0-1.5 x 10^6 cells per 30 mm plastic petri dishes. Serum starvation for G0 phase arrest, 2 mM-hydroxyurea treatment for G1/S phase arrest or 10 μM colchicine for G2 phase arrest was employed. All treatments lasted for 24 hours.

2.2. Generation of Plasmid Constructs.

2.2.1. DTL constructs—DTL cDNA was cloned into pBLUESCRIPT vector (Udvardi et al.). B-DTLup construct was made by inserting 681bp long KpnI-EcoRI cDNA fragment into Bluescript SK vector into the same restriction sites. For expression in pET-3 vector system, KpnI site was polished with T4 DNA polymerase to form a blunt end and an NdeI linker was inserted to this site. Then 699bp long NdeI-BamHI fragment was inserted into the pET-3 vector at the same restriction sites.

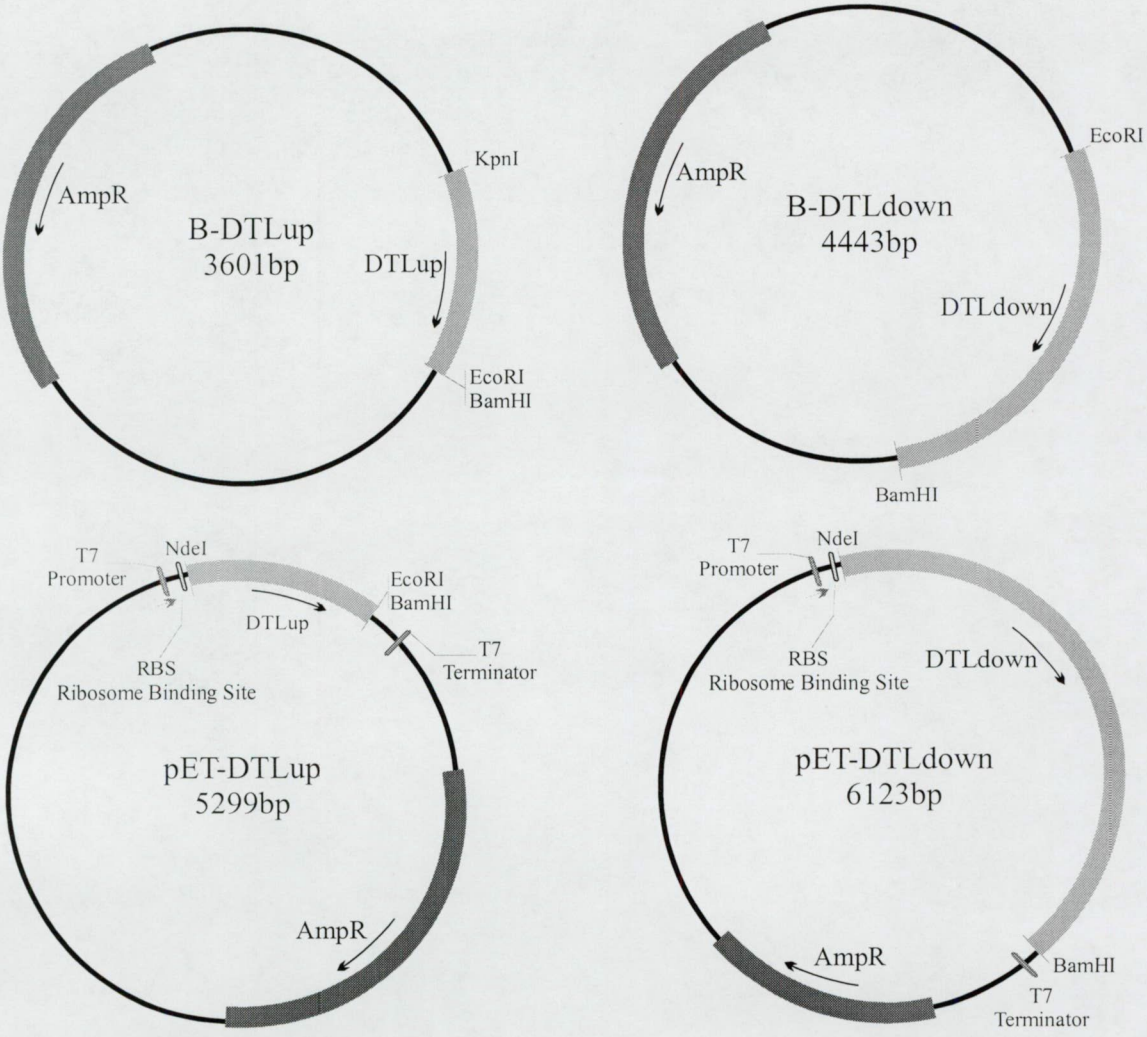

A. DTL constructs

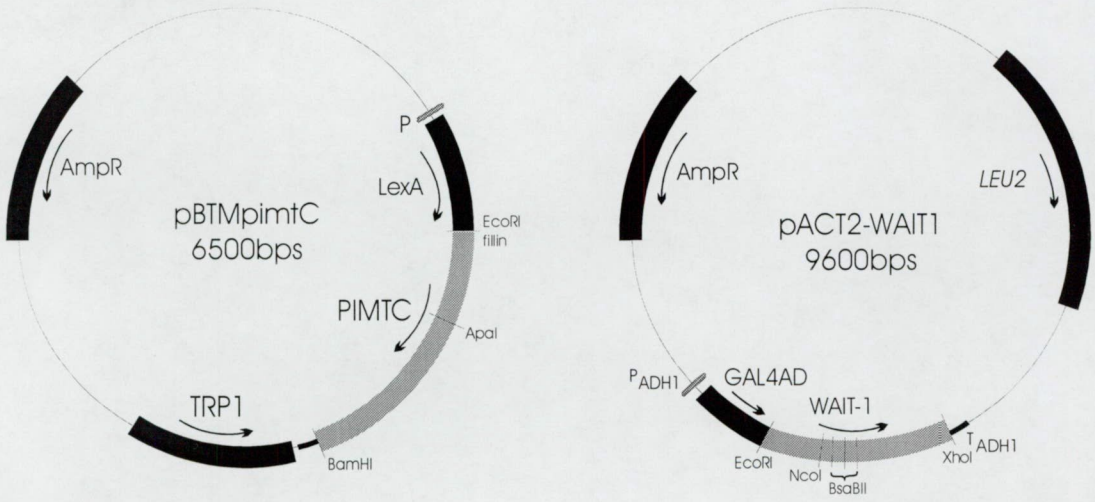

B. Yeast two hybrid constructs

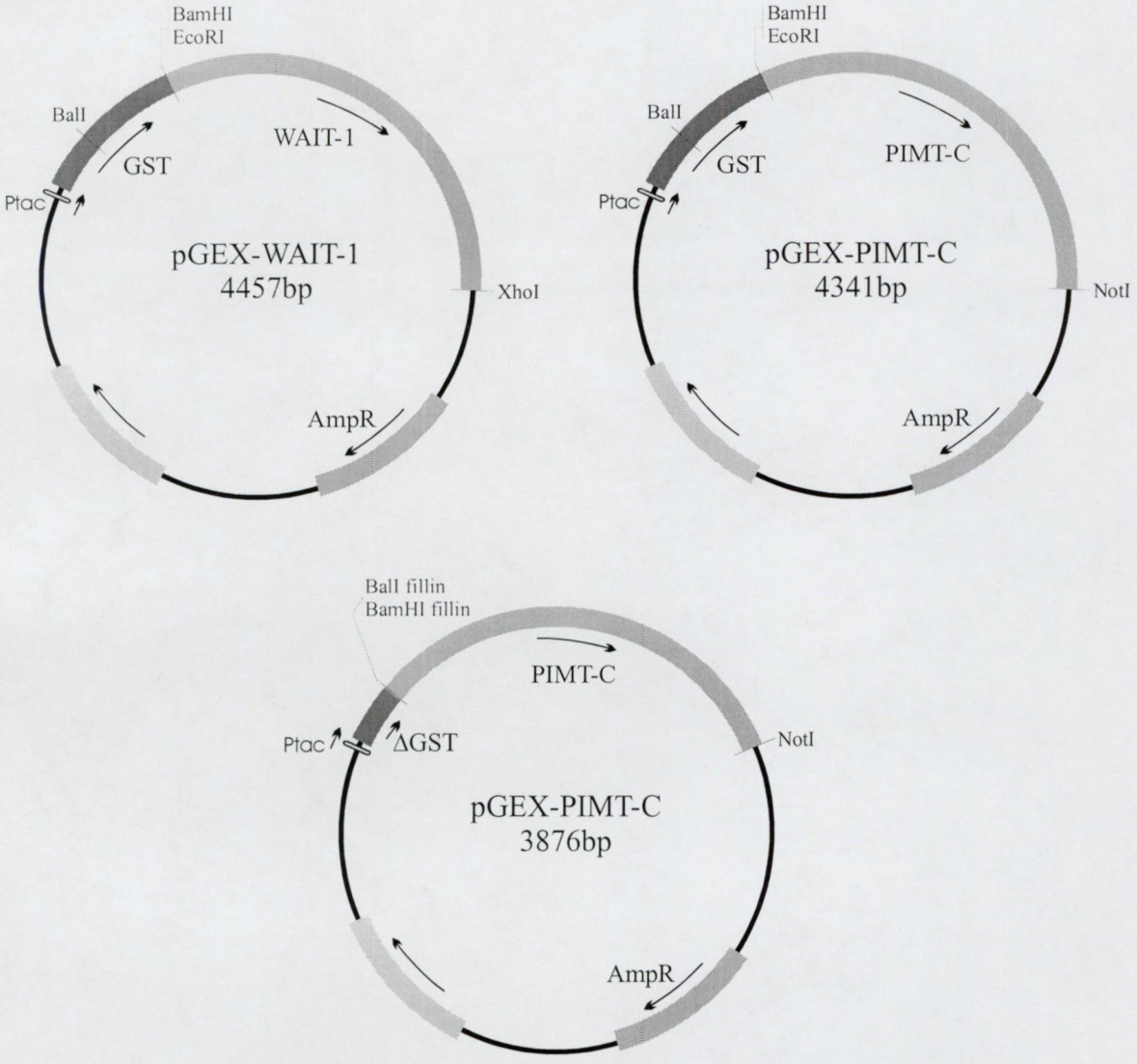

C. In vitro pull down constructs

Figure 1. Schematic drawing of the main plasmids used in this work.

B-DTLdown construct was made by inserting 1523bp long EcoRI-BamHI cDNA fragment into the same sites in Bluescript SK vector. Then EcoRI site was treated with Kleenow fragment and an NdeI linker was inserted to the blunt-ended site. To express full length cDNA in pET vector system, 1523bp long EcoRI-BamHI fragment from B-DTLdown was inserted to the same sites of pET-DTLup construct (Figure 1A).

2.2.2. LexA-PIMT-C Bait—The partial mRNA sequence coding from amino acid 555 to 852 of PIMT was purchased as an EST sequence (GenBank Accession No.AA174934). This sequence was cloned into BTM116 vector between EcoRI and BamHI sites. To correct the frame in order to produce a fusion with DNA binding LexA gene, EcoRI site was digested and filled in with DNA polymerase Kleenow fragment (Figure 1B).

2.2.3. WAIT-1 Mutants—WAIT-1 mutant plasmid constructs for the yeast two hybrid interaction assay were done on the original pACT-WAIT-1 clone which was isolated by a yeast two hybrid screen. pWAIT-1dc clone was constructed by partial digestion with NcoI, pWAIT-1dn clone was constructed by full NcoI digestion, and for pWAIT-1dwd and dwd2, pACT-WAIT-1 was linearized with XhoI and BsaBI, respectively, then pWAIT-1dwd was shortened by BAL31 digestion. All restricted and modified constructs were filled in and re-ligated (Figure 1B).

2.2.4. Fusion Protein Constructs-- pGEX-WAIT-1 was constructed from the sequence retrieved from yeast two hybrid screen as a fusion to GST protein in pGEX-4t vector. For this purpose 1557bp long EcoRI-XhoI fragment was inserted to the same site in pGEX-4t-2 plasmid. 1419bp long EcoRI-NotI PIMT-C (from 555 amino acid to 853) protein was also cloned into pGEX-4t-2 plasmid as a fusion protein. For *in vitro* binding experiments GST protein coding sequence was removed from the construct with BamHI-BalI digestion, then filled in and religated. This construct carried just 80 amino acids of the GST protein, which does not have affinity for glutathione (Figure 2).

2.3. Antibodies

DTL related antibodies were raised in rabbit by injecting bacterially expressed and PAGE purified proteins. Synthetic peptide EIPNSPHATEVEIK was injected to rabbit to raise antibody against PIMT. Antiserum was collected and further purified by affinity chromatography. The truncated PIMT-C protein was bound to GST-sepharose beads (Amersham-Pharmacia). GST fusion protein was purified and eluted according to Pharmacia manual. His-tagged DTL protein was purified by IMAC (immobilized methal affinity chromatography) by using a Ni^{2+} resin. Purified proteins were bound to CnBr activated sepharose (Amersham-Pharmacia) according to manufacturer's instructions. Anti-sera was added to 1:20 dilution and incubated at RT for 3-4 h. After extensive washing with PBS, bound antibodies were eluted with 100 mM glycine/HCl pH 2.5 for 5 min and immediately neutralized with the addition of 1:10 of the elution volume of 1 M Tris pH 8.0.

2.4. Rubidium Chloride method for Transformation of Competent *E. coli*

1 ml from overnight culture of appropriate *E. coli* strain was inoculated into 100 ml LB media. Culture was incubate at 37°C water bath while shaking to OD_{550nm}=0.5. Culture media was cooled down on ice for 15 min. Cells were centrifuged at 5000 rpm for 10 min using a Sorvall SS-34 rotor. Supernatant was discarded and 0.4 volume (i.e. of original volume) Buffer I (30mM potassium acetate, 100 mM Rubidium Chloride, 10 mM calcium chloride, 50 mM manganese chloride, 15 %v/v glycerol) was added, and the pellet was resuspended. Cells were incubated on ice for 15 min and pelleted as before. Supernatant was discarded and the pellet was resuspended in 0.16 volume Buffer II (10 mM MOPS, 75 mM $CaCl_2$, 10 mM $RuCl_2$, 15 %v/v glycerol). The cells were incubated on ice for 15 min and either used immediately or aliquoted

and quick frozen at -70°C for storage. Typically 200 µl of cells were transformed with 4-5 µl of a ligation reaction.

2.5. Yeast Techniques

2.5.1. Transformation of yeast cells--Using a single colony of *S. cerevisiae* strain L40, 10 ml of YPD media (10 g yeast extract, 20 g peptone, and 20 g dextrose) were inoculated and shaken overnight at 30°C. Overnight culture was diluted into 50 ml YPD at 30°C and incubated a further 3hrs.

The cells were pelleted by centrifuging at 1000g for 3min and gently resuspended in 1 ml of sterile TE/LiA. For each transformation 0.5 mg plasmid DNA from bait and/or prey constructs, 10 µg sonicated salmon sperm DNA and 100 µL of yeast cell suspension were mixed in a 1.5 ml microcentrifuge tube. 600 µL of PEG/LiAc solution was added and mixed gently. Then tubes were placed in a 30°C incubator for 30 min. At the end of incubation, 70 µL DMSO was added to each transformation and heat shocked at 42°C for 6-7 min. Cells were pelletted by spinning briefly, then resuspended in 100 µL TE and plated out onto selective plates. Selective minimal media TULLH was composed of 1.2 g yeast nitrogen base without amino acids (DIFCO), 5g $(NH_4)_2SO_4$, 10 g succinic acid (Sigma), 6 g NaOH, 0.55 g CSM (complete supplement mixture without Trp, Ura, Lys, Leu, His) BIO101, 0.1 g adenine (Sigma), 20% glucose in 1 liter. For solid media 20 g agar was added per liter of media.

2.5.2. Yeast two hybrid screen-- pACT cDNA libarary (Clontech) was screened with yeast two-hybrid method, using pBTM-PIMT-C as a bait. *S. cerevisiae* strain L40 was transformed with pBTM-PIMT-C as described above. Transformed mixture was plated on TUL media (0.1 g Leu, 0.05 g His were added to TULLH media). A single positive colony was used to inoculate 5 ml of TUL drop-out media. The culture was twice expanded in two days to reach a 300 ml volume

OD_{600nm}=0.6. Then cells were harvested in sterilized GSA bottles by centrifuging at 5000 rpm for 10 min . The pellet was washed with 500 ml sterile water, and resuspended in 20 ml TE/LiAc solution (50 mM Tris-HCl pH 7.5, 0.1 M Li-acetate, 5 mM EDTA). Cells were transferred into a 250 ml flask and 1 ml 10 mg/ml denatured salmon sperm DNA, 400 mg pACT cDNA library DNA, and 140 ml PEG/LiAc solution (50 mM Tris-HCl pH 7.5, 0.1 M Li-acetate 40% PEG-3350, 5 mM EDTA) was added. The transformation mixture was shaken at 30°C for 30 min. The mixture was transferred to a 2 liter flask, then 17.6 ml dimethyl sulfoxide (DMSO) was added and heat shocked for 8 min while swirling the flask. Then the flask was cooled down by flushing outside with tap water. Cells were pelleted at 5000 rpm, for 10 min, resuspended in 1 liter YPD media and were grown for 1 hour to allow expression of genes. Cells were pelleted and resuspend in 1 liter TULLH media (0.05 g His added to TULL media). After 4 hours of incubation at 30°C cells were pelleted , resuspended in 10 ml TULLH media and plated out on agar plates of the same media. Emerging colonies were transferred into replica plates, and colonies from one of the plates were transferred onto nitrocellulose filters, and further tested for their β-galactosidase activity.

2.5.3. Recovery of positive plasmids—The positive yeast colonies, which carry both bait and prey vectors, were grown in 5 ml liquid histidine, leucine, and tryptophan deficient minimal yeast media overnight in 30°C heated water bath by shaking 250-300 rpm. The cells were pelletted by centrifuging at 1000 rpm for 3min. The cells were resuspended in 1 ml sterile water, and pelleted as before. Then cells were resuspended in 100 μl lysis buffer (50 mM Tris-HCl pH 7.5, 10 mM EDTA, 0.3% β-mercaptaethanol, 1 mg/ml Zymolase(Sigma)). The mixture was incubated in 37°C water bath for 1 hour. After the incubation was complete the cells were lysed by the addition of 20 μl 10% SDS. 100 μl 7M ammonium acetate was added and the lysate was placed in dry ice for

15 min. The cell debris were precipitated by centrifuging at 13000rpm for 15 min. Supernatant was transferred to a clean 1.5 ml Eppendorf tube and the plasmid DNA was precipitated with 0.7 volume isopropanol by placing on dry ice for 15 min. Plasmid DNA was pelletted by centrifuging at 13000 rpm for 15 min. DNA pellet was washed with 70% ethanol and dissolved in 20 µl TE/1mg/ml RNase. 5 µl DNA was used to transform *Escherichia coli* HB101 cells that were plated on M9/amp/-leu to selectively rescue only activation domain (AD)/ library plasmids.

2.5.4. **β-galactosidase assay--** The strength of the interaction between the various deletion mutants of PIMTC and WAIT-1 was determined by measuring the expression level of the lacZ reporter gene in liquid culture. The β-galactosidase activity was determined according to the general methods (Maniatis et al.35). For solution assays, yeast cells that contained different sets of plasmids were cultured overnight in yeast synthetic media that contained 2% of histidine. 1 ml of the culture broth was aliquoted and cells were pelleted. Pellet was frozen in liquid nitrogen and thawed for cell lysis, and then resuspended in 0.3 ml Z buffer that contained 2-β-mercapto-ethanol. The reaction was started by adding the substrate o-nitrophenyl β-D-galactopyranoside (ONPG) (8 mg/ml) (0.2 ml), incubated at 30°C until the yellow color appeared, and then stopped by adding 0.4 ml of 1 M Na2CO3. Cell debris was removed by centrifugation. The absorbency of the supernatant was measured at 420 nm.

2.6. *In Vitro* Binding Assays

WAIT-1 protein was bacterially over expressed in *Escherichia coli* BL21 cell line as glutathione S-transferase (GST) fusion proteins, using the pGEX-4t plasmid (Amersham Pharmacia Biotech). WAIT-1-GST fusion protein was purified by affinity chromatography on glutathione-Sepharose gel (Amersham Pharmacia Biotech). For in vitro interactions, 250 µl aliquots of glutathione-Sepharose bead suspension were mixed with 5 ml aliquots of sonicated

bacterial cell lysate (corresponding to 250 ml of E. coli culture) in binding buffer (BB: phosphate-buffered saline, containing 1% TritonX100 and 1mM PMSF) and incubated for 1 h at RT. After extensive washing in BB, 20 µl aliquots of the affinity beads were mixed with 1000 µl of sonicated bacterial lysate of PIMT-C expression (corresponding to 50 ml of E. coli culture) and incubated for 2 h at room temperature. The beads were then washed three times with 1000 µl of BB, resuspended, and boiled in 50 µl of SDS sample buffer. GST protein alone was processed parallel as a negative control. Eluted proteins were analyzed by SDS-polyacrylamide gel electrophoresis (SDS-PAGE) and immunoblotting.

2.7. Preparation of protein samples

2.7.1. Bacterial expressions: Bacteria which express recombinant protein were pelleted and resuspended in lysis buffer. After freezing in -70°C for one hour, cells were allowed to thaw on ice slowly. Then the cell suspension was sonicated and protein concentration was quantified either by SDS-PAGE or Bradford protein assay. Lysates were kept frozen at -80°C till further use.

2.7.2. Preparation of Animal Tissue Samples: Indicated organs were frozen immediately in liquid nitrogen upon removal from animals and they were stored at -70°C until protein extraction. Tissues were washed twice in ice cold PBS and extracts were homogenized in Extraction Buffer (10 mM HEPES (pH 7.9), 10 mM KCl, 0.1 mM EDTA, 0.5 mM DTT, 0.5 mM PMSF). Tissue extracts were immediately aliquoted and frozen in liquid nitrogen and kept at -80°C till further use.

2.7.3. Nuclear and Cytoplasmic Protein Fractionation of the Cells: Mammalian HeLa and *Drosophila* S2 cells were cultured in 25 cm^2 flasks, were washed twice with PBS and harvested in 3 ml of PBS per flask. Cells were pelleted and resuspended in 5 times pellet volume of ice cold Buffer A (10 mM HEPES pH 7.9, 10 mM KCl, 0.5 mM DTT, 0.5 mM PMSF) and incubated

on ice for 15 min. 25 µl 10% NP40 was added and vortexed for 10 sec. Nuclear fraction was pelletted by centrifugation at 3000 rpm for 5 min and supernatant was kept as cytoplasmic fraction. Pellet was resuspended in 5 times pellet volume of Buffer B (0.42 M KCl, 20 mM Tris pH 7.8, 1.5 mM MgCl2, 10% sucrose, 2 mM DTT, 0.5 mM PMSF) and incubated on ice for 30 min. Nuclei were sonicated for 15 sec.

2.7.4. Gel Electrophoresis and Immunological Procedures: The SDS-denaturing polyacrylamide gel electrophoresis for size fractionation of the total proteins was performed according to standard protocols (35).

Equal amounts of protein samples in SDS loading buffer were resolved by SDS-PAGE and analyzed by immunoblotting. A wide range prestained molecular weight marker was also run with the samples. For SDS-PAGE 120V of constant current was applied until the dye reached the bottom edge, typically within 1.5 hr. Before transfering the proteins onto nitrocellulose filters, the stacking gel was removed. Transfer of proteins onto nitrocellulose filters was done using an electroblotting apparatus (Bio-Rad, USA) in transfer buffer (39 mM glycine, 48 mM tris base pH 8.0).

Immunoblots were incubated with antibody against PIMT (1:7000), or against DTLup and DTLdown (1:6000) overnight at 4°C. Secondary antibody was diluted 10000 fold and incubated for 1 hour at room temperature. The immunocomplexes were visualized by the chemiluminescence. For the control blots, the preimmune sera was diluted at the same ratio like the immune sera. For competition assay purified GST-PIMT-C protein bound to glutathione sepharose was added to the anti-PIMT TBST solution (equivalent to 150 µl liquid media per 1 ml) .

2.8. Immunolocalization

HeLa cells were fixed on coverslips with 4% paraformaldehyde in PBS for 20min at RT. After washing, cells were permeabilized with 0.3% Triton-X-100 in PBS for 20 min. Schneider S2 cells were fixed on cover slips with 2% paraformaldehyde in PBS for 30 min at room temperature. After washing cells were permeabilized with 0.1% Triton-X-100 in PBS for 10 min. Unspecific sites were blocked with 5% BSA in in PBS for 1 hour. Cells were incubated with rat polyclonal anti-tubulin (YOL1/34, Sera Labs, Sussex, UK), and rabbit polyclonal anti-PIMT antibodies in 1:200 dilution for 2h at 23°C. TRITC (tetramethyl rhodamine isothiocyanate) or FITC (fluorescein isothiocyanate)-labelled secondary antibodies (Sigma) were used. Nuclei were stained with DAPI (4', 6-diamidino-2-phenylindole HCl) (100ng/ml) and cells were mounted with Citifluor (Ted Pella Inc. CA, USA).

Control experiments excluding the fluorescent primary antibody or replacing the primary antibody with non-immunized serum were performed for all the immunolocalization experiments.

2.8.1. Immunofluorescence Microscopy: Cytological analyses were done using a Nikon Eclipse TE300 fluorescence microscope equipped with SPOT RT CCD camera (Diagnostic Instruments Inc. MI, USA). To reach the maximum possible magnification and resolution, majority of the observations has been captured using oil-immersion Plan Apo 60x /1.40 objective. Saved pictures were colored in RGB format.

2.9. Flow cytometry

HeLa cells were trypsinized and washed twice. After the last wash, the cells were fixed and permeabilized with ice cold 70% ethanol on ice for 20 min. Cells were centrifuged at 3000 rpm for 5 min and resuspended in staining buffer (0.1% sodium citrate, 0.1% TritonX100, 10μg/ml Propidium Iodide (PI) and 10μg/ml RNase) for 30 min. PI is a double stranded nucleic

acid binding fluorochrome that intercalates in the double-helix. Ribonuclease-A was used to eliminate the staining of double-stranded RNA. Measurements were evaluated by WinMDI and Cylcred software and represented as the percentage of the cells in G1, S and G2 phases.

2.10. Synthesis of siRNAs

SiRNAs were designed and synthesized according to the criteria and procedure published by Donzé et al. (36). The following oligo nucleotides were used for the synthesis of siRNAs specific to PIMT mRNA:

T7 promoter complementary oligonucleotide 5'-TAATACGACTCACTATAG-3'; PIMT nucleotides 626-630 relative to the initial methionine: sense, 5'-TGGTGAACTTGAAACAGAAAACTATAGTGAGTCGTATTA-3'; antisense, 5'-ATGTTTTCTGTTTCAAGTTCACTATAGTGAGTCGTATTA-3'.

3. RESULTS

3.1. Drosophila TAT Like protein (DTL)

3.1.1. *dtl* gene encodes an RNA binding protein with a methyltransfearse domain

In a screen cDNA fragments of a protein with RNA binding specificity similar to those of Human Immunodeficiency Virus (HIV) TAT transactivator protein are isolated by Udvardy et.al. (personal communication)

Since in this screen, TAR (Transactivation Response RNA element) RNA of HIV was used as a bait the cDNA fragment representing a so far unknown gene designated as *dtl* (Drosophila Tat Like) gene was isolated. The transcript of *dtl* had an interesting structure having two open reading frames (ORFs). The stop codon of the first ORF with one base shift towards 5'-end is the start codon of a second longer ORF which codes the RNA binding protein recovered from the screen. The first ORF (DTLup) is 184 amino acids and the down stream ORF (DTLdown) is 491 amino acids long.

To identify functional domains through conserved domains of homologous proteins, database search was performed. This search revealed that DTLdown had several homologues in different species extending from yeast to human. These proteins shared a well conserved C-terminal domain, which was similar to methyltransferases (Figure 2A). The most conserved motifs found in similar methylase domains were a 9-amino acids methyltransferase Motif I (VVDAFCGVG), a 7-amino acids Motif II (KADVVFL), and an S-adenosyl-L-methionine interacting region (Figure 2B). Conserved domains were not found in the upstream ORF. However, in the upstream ORF a leucine rich domain was shown to be a potential leucine zipper motif by several search engines.

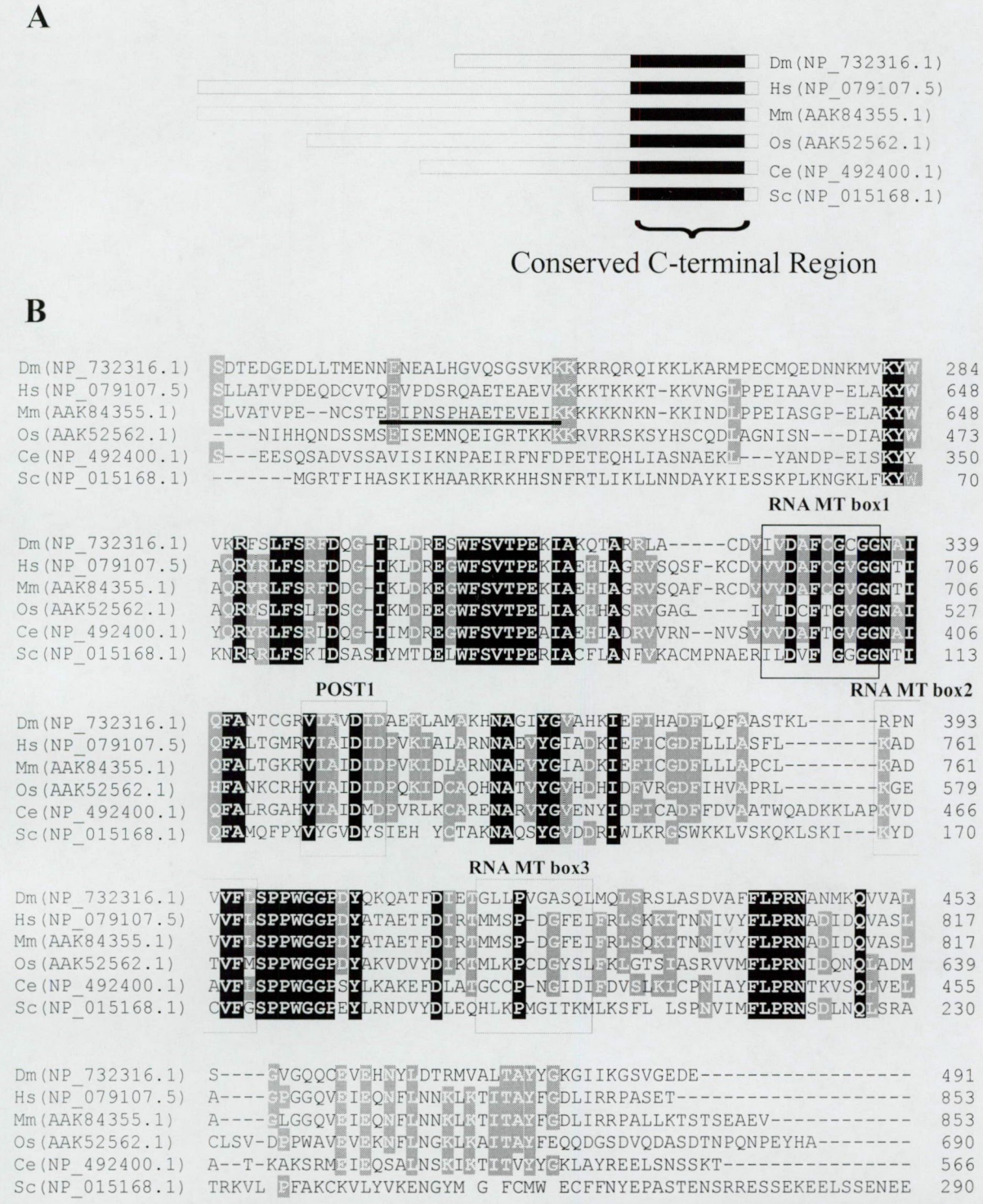

Figure 2 Alignment of DTL-related putative protein sequences with methyl-transferase domain from different organisms

A. DTL homologues are conserved through their C-terminal. DTL homologue amino acid sequences from various species were extracted from the GenBank, EMBL, DDBJ and Genome Sequencing Center databases by iterative searches using the standard BLAST program and DTL as query. The amino acid one-letter code is used. The various DTL-related sequences are as follows: *Drosophila melanogaster* (Dm) DTL (CG31241-PA) (Accession N°: NP_732316.1), *Homo sapiens* (Hs) PIMT (Accession N°: NP_079107.5), *Mus musculus* (Mm) (Accession N°: AAK84355.1), *Oryza sativa* (Os) (Accession N°: AAK52562.1), *Caenorhabditis elegans* (Ce) T08G11.4.p (Accession N°: NP_492400.1), *Saccharomyces cerevisiae* (Sc) Ypl157wp (Accession N°: NP_015168.1).

B. Conserved C-terminal regions of DTL homologues. Multiple alignment was performed with Multalign program. Residues conserved amongst all DTL homologues have a black background; residues conserved in 4 out of 6 of the homologues have a light gray background. The highly conserved RNA methyl-transferase (RNA MT) domains and S-adenosyl-L-methionine interacting region (POST1) are boxed [1]. Peptide stretch for the antibody target is underlined.

3.1.2. Preparation of DTL specific polyclonal antibodies

In order to perform *in vitro* studies, polyclonal antibodies were raised against the recombinant proteins expressed from the two ORFs of DTL. For this purpose, each of the two open reading frames were cloned into pET vector separately for bacterial expression (Figure 3A). pET-DTLup construct could express entire 184 amino acids of DTL upstream ORF. pET-DTLdown construct could express only N-terminal truncated 423 amino acids long partial DTL down stream ORF.

These recombinant proteins were expressed in DE3 *E. coli* strain and the cell extracts were examined on SDS-PAGE. As expected from theoretical calculations of amino acid composition, pET-DTLup construct expressed an approximately 20 kDa protein and pET-DTLdown construct expressed an approximately 50 kDa protein in bacteria.

The bands belonging to the recombinant proteins were excised from preparative SDS-PAGE, and used to raise polyclonal antibodies in rabbit (Figure 3B). The specificity of the immune sera was tested against DTLup or DTLdown bacterial expressions. The polyclonal antibodies recognized specifically their target proteins expressed in bacteria (Figure 3C).

3.1.3. Only down stream ORF of *dtl* gene was translated in Schneider S2 cell line

As it is mentioned earlier, the cDNA of *dtl* gene coded two open reading frames. Since DTLdown had RNA binding property and also conserved methylase domains, it was thought to be a translated unit. However, DTLup had no conserved regions except a potential leucine zipper motif identified by several databases. Therefore, we decided to determine if the leucine zipper motif was functional in the translated protein.

Bacterially expressed DTLup proteins were resolved on denaturing and non-denaturing PAGE and blotted by DTLup polyclonal antibodies. Under non-denaturing conditions 20, 40, and 80 kDa bands could be recognized. However under denaturing conditions 40 and 80 kDa bands were not observed. That showed that 40 and 80 kDa proteins observed under denaturing conditions are homodimers, and tetramers of DTLup respectively. That prooved that leucine zipper motif is a real functional structure for the upstream ORF (Figure 4). The existence of a functional domain in DTLup strenghtened the possibility that DTL upstream ORF also was a translated unit. Therefore it could be thought that two open reading frames of *dtl* gene were actually translated as a single protein with a ribosomal shift during protein translation. Moreover, this protein might homodimerize through DTLup, bind RNA and possibly methylate RNA through DTLdown.

It is known that some eukaryotic ribosomal shift signals can be recognized by the bacterial ribosome (37). Therefore, to test the idea that ribosome may shift from upstream to downstream ORF keeping the continuity of the translated protein whole cDNA fragment was inserted into a pET vector system. The missing 3′-end of the DTL transcript was added to pET-DTLup construct and expressed in DE3 *E. coli* strain (Figure 5A). Cell extracts were blotted with either up-, or down-stream specific polyclonal antibodies raised and tested previously. It was observed that two ORFs were translated simultaneously as two separate proteins (Figure 5B).

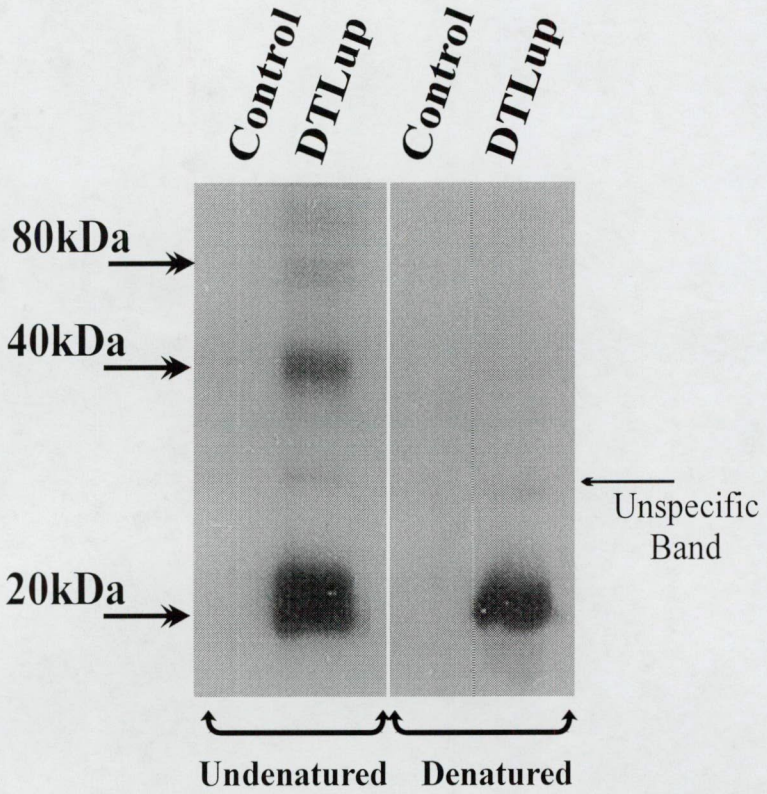

Figure 4. Leucine zipper motif of the DTLup

We interpreted the presence of a leucine rich region as a sign for a leucine zipper motif for dimerization of the DTLup protein. To check this possibility bacterially expressed protein were denatured as usual with SDS and heat for control. Experimented sample was kept in a less harsh environment (free from heat and SDS) to keep some of the features of the native folding. Both samples were run on SDS-PAGE, and blotted with DTLup antisera. *E. coli* DE3 cell extracts were used as control. Western blot showed that undenatured sample formed homodimers and tetramers as expected from a leucine zipper motif.

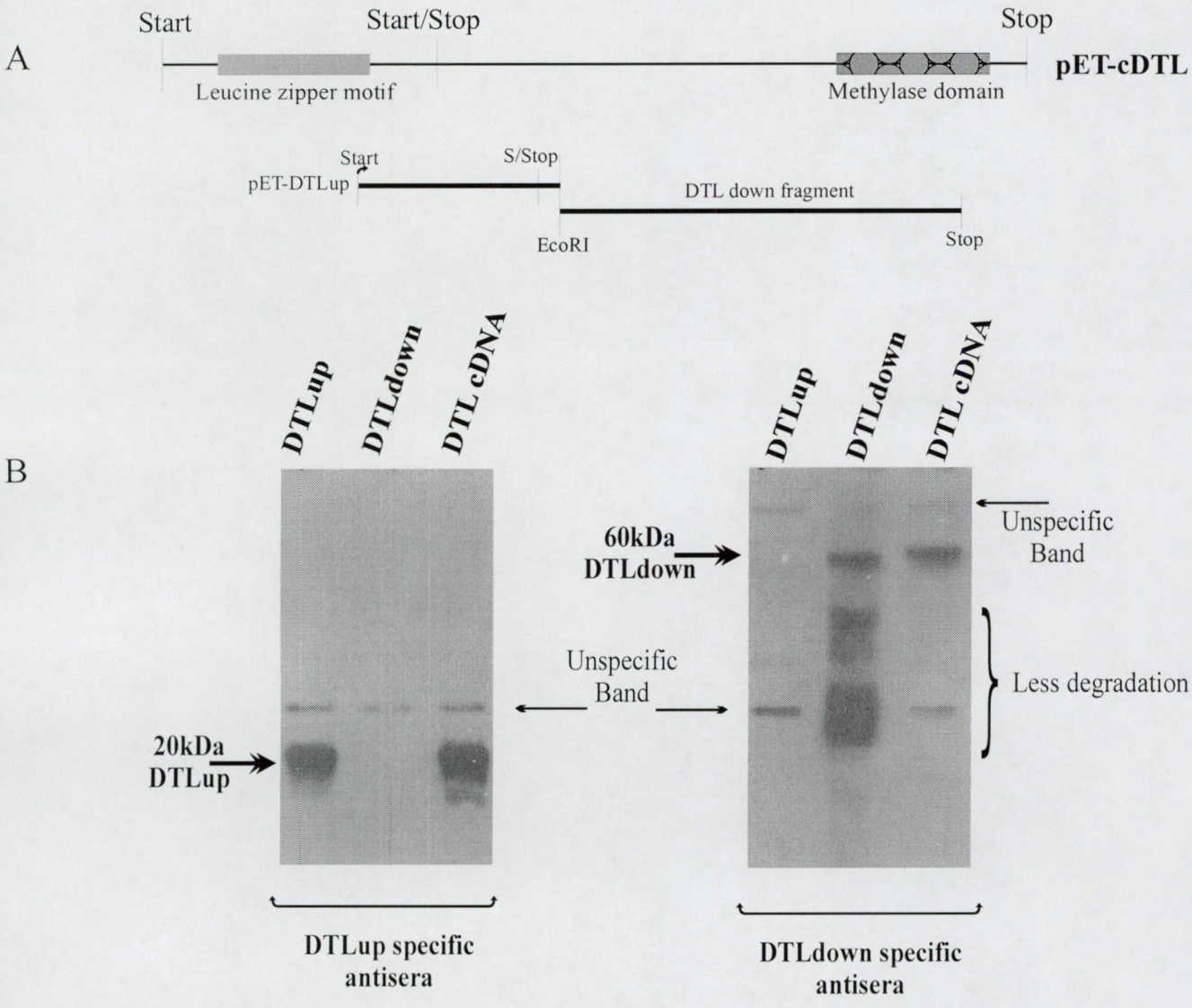

Figure 5. DTL cDNA in pET vector

A. To express whole cDNA in bacteria the missing DTLdown ORF sequence was inserted under the pET-DTLup construct. The new construct had initiation codon for the DTLup protein, and ATGA start/stop sequence residing in the beginning of the second ORF was to test the ribosomal shift assay.

B. pET-cDTL bacterial expression was blotted with both DTLup and DTLdown antisera. It was seen that both ORF were co-expressed from the cDNA as two separate proteins, failing the hypothesized ribosomal shift in bacterial ribosome. However the second initiation codon resulted a more stable protein from the second ORF.

Although translations of polycistronic messages in bacterial systems are common, recognition of initiation codon of DTLdown ORF suggested an internal ribosomal entry site in eukaryotic translation machinary. It was also seen that the translated protein from this internal methionine was more stable than the amino terminal truncated version of the same protein (Figure 5B).

To identify DTL proteins translated in *Drosophila*, Schneider S2 cell line extracts were blotted by polyclonal antibodies raised against the DTLup and DTLdown proteins. Antisera of two rabbits, which were immunized against the recombinant DTLdown protein were purified for their affinity to DTLdown protein to enhance their specificity. Total protein extracts of the S2 cells were blotted by these polyclonal antibodies and two specific bands with molecular weight of ~60 kDa and ~120 kDa were observed by both anti-DTLdown antibodies (Figure 6A). On the other hand, DTLup polyclonal antibodies exhibitted a lower specifity on blots of S2 cell extracts and did not recognize any band on the 60 and 120 kDa range. That showed that DTL was translated from an internal ribosomal entry site using only donwn stream ORF (DTLdown) in Schneider S2 cells.

3.1.4. DTL localizes in the cytoplasm in the Schneider S2 cell line

Affinity purified polyclonal antibodies specific to DTLdown were used to determine the localization of the DTL protein in *Drosophila* S2 cell line. S2 cells were fractionated into their cytoplasmic and nuclear components and blotted. Western blots showed that both isoforms of DTL were cytoplasmic proteins (Figure 6B).

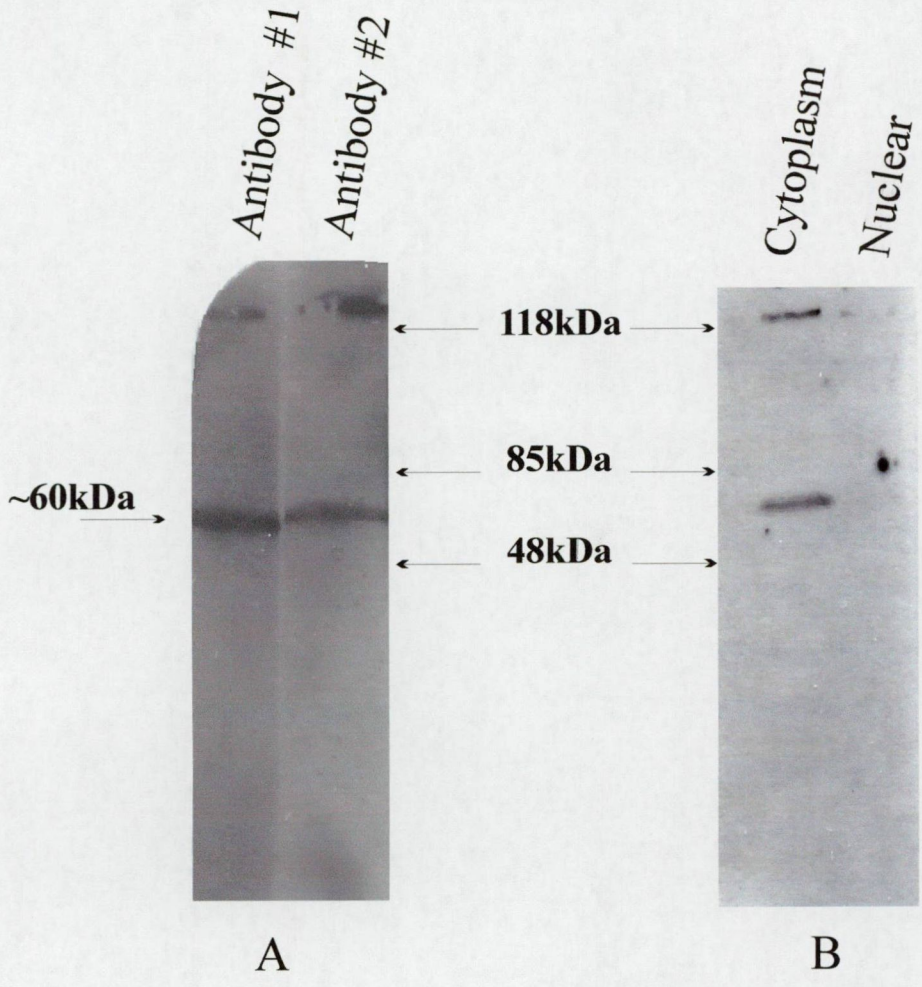

Figure 6. Detection of DTL in *Drosophila* S2 cells

A. *Drosophila* S2 cell extracts were blotted with affinity purified DTLdown specific antibodies. Two specific bands could be distinguished by both antibody. One of expected size ~60 kDa, and a second a much larger ~120 kDa protein.

B. S2 cells were fractionated to their cytoplasmic and nuclear parts, and blotted with one of the affinity purified DTLdown specific antibody. The 60 and 120 kDa proteins were detected in the cytoplasmic fraction.

Figure 7A

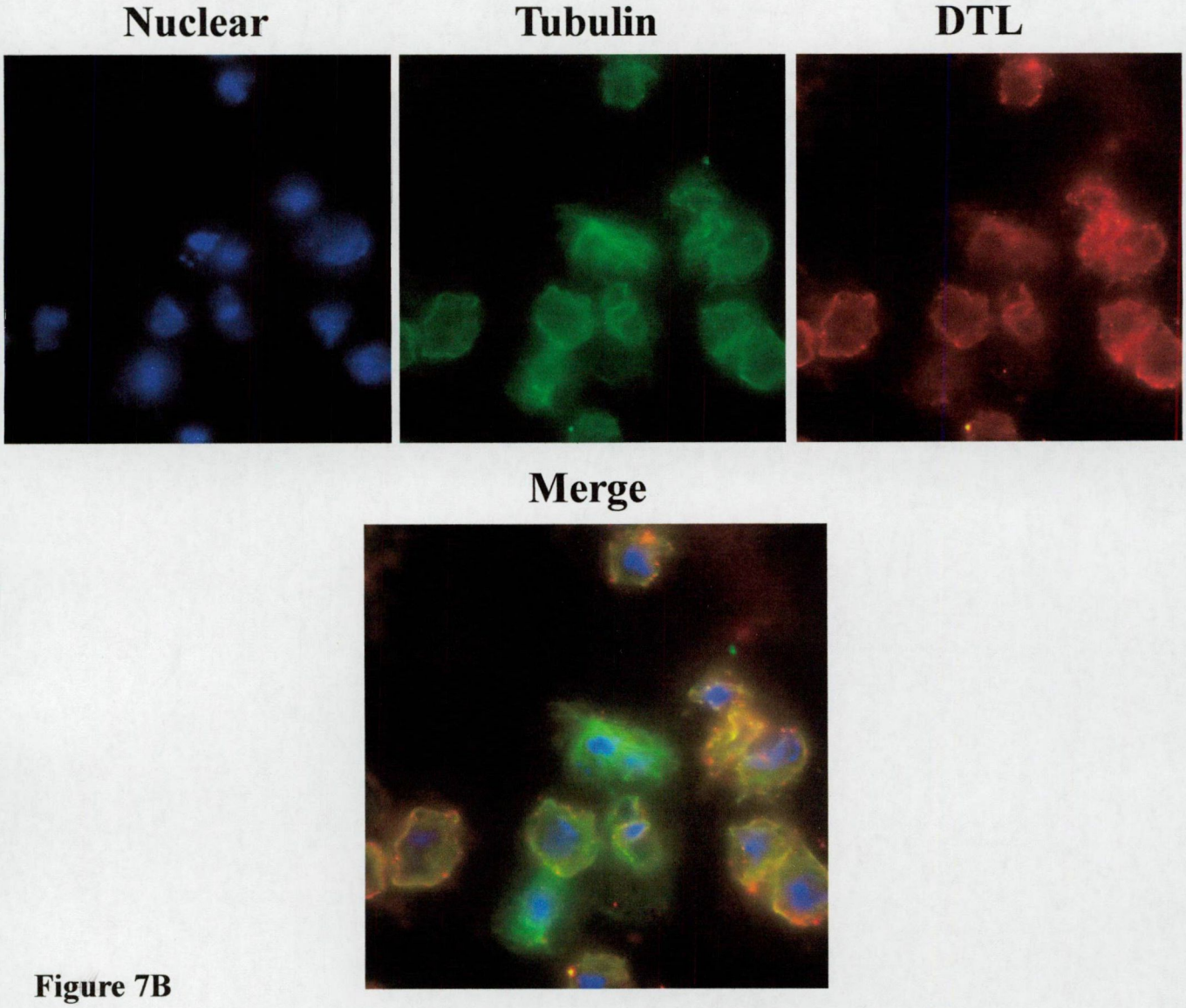

Figure 7B

Figure 7. Immunolocalization of DTL in Schneider cells

Two DTL specific antisera were purified by their affinity against bacterially expressed DTLdown protein. Figure A and B represents DTL localization by these two different antisera. For double immunolocalization mouse tubulin antibody was used together with rabbit DTL antibodies. Anti-mouse (Rhodamine), anti-rabbit (FITC) was used as secondary antibodies to detect DTL and tubulin structures, nuclear DNA were stained with DAPI. In the images DTL signal was represented with red, tubulin with green and nuclear DNA with blue. It is seen that DTL localization is cytoplasmic and in the merged images DTL distribution is on the microtubule cytoskeleton as overlapping green and red patterns turn yellow. Moreover the levels of DTL expression appear to change at different cell cycle phases.

The same antibodies were used to immunolocalize DTL in S2 cells. To simplify perception mouse anti-tubulin antibody was used together with rabbit anti-DTL antibodies. Double immunolocalization revealed that DTL was co-localized with microtubule cytoskeleton (Figure 7). The co-localization can be deduced by tubulin (red) and DTL (green) signals merged to produce yellow color in composite pictures. These pictures also showed that expression level DTL was not constant during cell cycle and was in its lowest during mitosis. However, its existence in cytoplasm co-localized together with the microtubule cytoskeleton was constant in all phases of cell cycle.

3.2. Mammalian homologue of DTL

3.2.1. Different isoforms of mammalian DTL exist

DTL was recovered through its interaction with a mammalian virus RNA. This is why to characterize mammalian homologue of DTL might support and clarify certain aspects of DTL. Since the amino acid similarities shared by DTL and its relatives were located in the C-terminal half of the homologues, a murine EST sequence with a high similarity to the C-terminal of DTL was purchased.

To facilitate *in vitro* studies polyclonal antibodies were raised against the 14 AA peptide: **EIPNSPHATEVEIK** , which corresponds to the amino acids 44 to 57 of the purchased EST sequence. Recently, mammalian homologues have been identified as PIMT (PRIP interacting protein with methyl transferase domain) (38). To prevent confusion of terminology, mammalian homologue of DTL will be named as PIMT and the EST sequence PIMT-C, because it also codes the whole C-terminal of PIMT protein (amino acids 555-852). The specificity of the raised antibody was tested on bacterially expressed PIMT-C and GST-PIMT-C fusion proteins by Western blots.

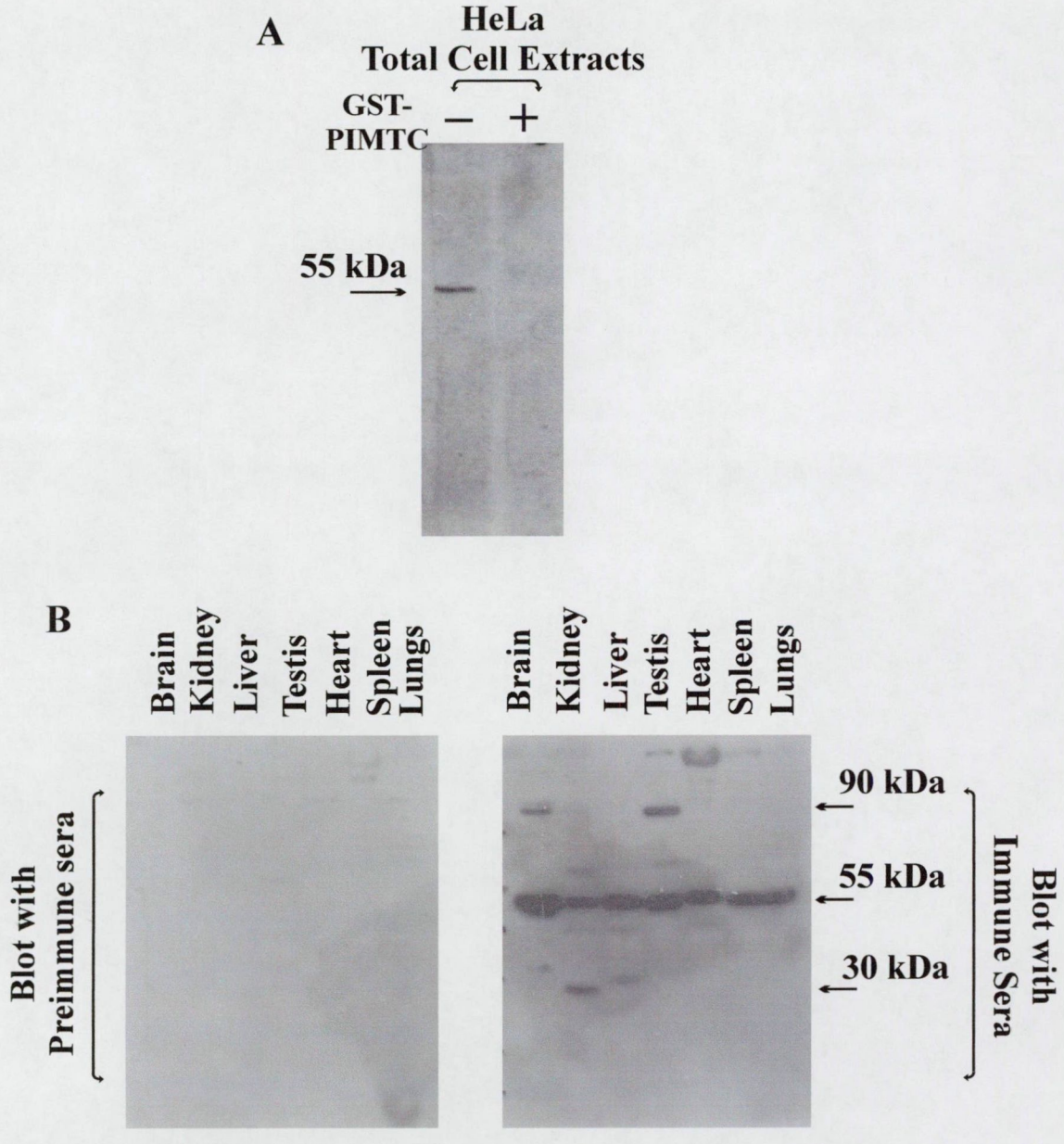

Figure 8. Human DTL antibody and different PIMT isoforms in mouse tissues

A. Competition experiments with bacterially expressed, purified GST-PIMTC protein to demonstrate the specificity of anti-PIMT antibody. HeLa total cell extracts were resolved on 10% SDS-PAGE and blotted with anti-PIMT polyclonal sera. On line "+" PIMT anti-sera were pre-incubated with sepharose-glutathione-bound purified GST-PIMTC as described in Materials and Methods.

B. 55-kDa PIMT protein expressed ubiquitously in rat. Protein extracts of different rat tissues as indicated were resolved on 10% SDS-PAGE and blotted with anti-PIMT antibody (Immune) or with pre-immune (Preimmune) sera taken from the same rabbit before immunization. Arrow indicates a ubiquitously expressed 55-kDa protein interacting specifically with PIMT-specific antibody. A 30-kDa protein present in kidney and a 90-kDa form present in brain and testis samples are also indicated.

Through antibody titration and competition experiments, we established that the raised antibody specifically recognized the C-terminal part of PIMT (Figure 8A).

To determine the tissue distribution of PIMT (mammalian DTL) protein, rat tissues were screened by Western blot analysis. Tissue homogenates were prepared from different rat tissues. Equal amounts of protein samples were resolved on SDS-PAGE and analyzed on Western blots. Immunoblots developed by anti-PIMT antibody showed three specific bands. A 55kDa protein was detected in all tissue samples examined, a 90-kDa protein was observed only in brain and testicular homogenates, whereas a much smaller, 30kDa protein was observed only in kidney homogenate. Probing the filter with pre-immune sera collected from the same rabbit before immunization did not reveal any protein interacting non-specifically (Figure 8B).

3.2.2. 55-kDa isoform of PIMT is a cytoplasmic protein that co-localizes with microtubule cytoskeleton

In HeLa cells, the anti-PIMT antibody recognized a single 55-kDa form of PIMT (Figure 9A). This shorter isoform was named as PIMT55. To determine the cellular localization of PIMT55, HeLa cells were fractionated into cytoplasmic and nuclear fractions and analyzed by Western blots. It was seen that the PIMT55 was a cytoplasmic protein as its *Drosophila* homologue DTL (Figure 9A).

To investigate the nature of the cytoplasmic localization of PIMT55, immunolocalization with anti-PIMT antibody was performed. The antiserum used in these experiments was affinity purified against bacterially expressed GST-PIMTC fusion protein. In fixed HeLa cells PIMT was detected in the cytoplasm showing a distribution similar to that of the microtubule cytoskeleton as in case of DTL (Figure 9B).

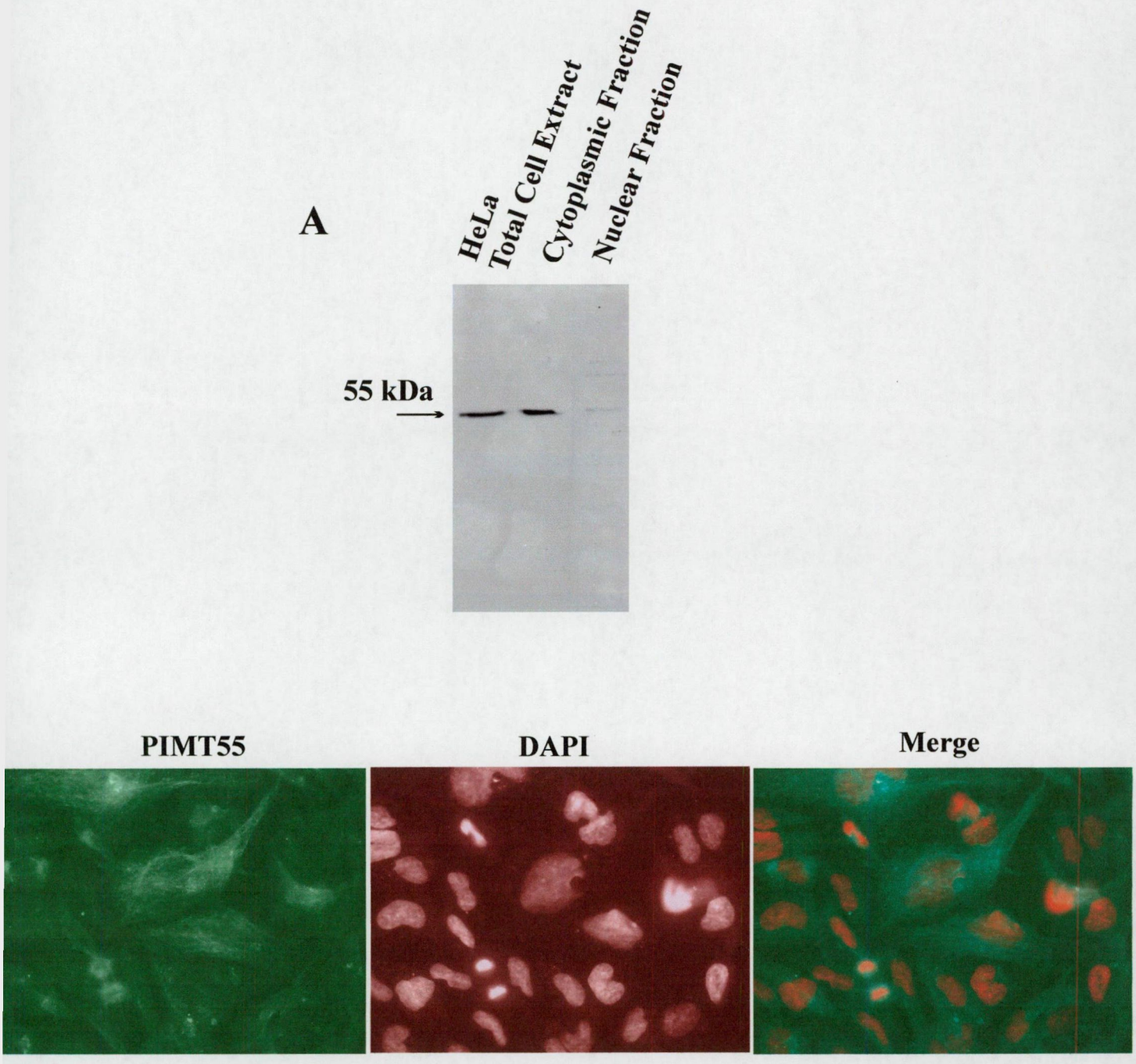

Figure 9. Localization of PIMT55 in HeLa cells

A. PIMT55 was localized to the cytoplasm in HeLa cell fractions. HeLa cells were separated to cytoplasmic and nuclear fractions and blotted with anti-PIMT antibody. The 55-kDa protein is seen exclusively in the cytoplasmic fraction.
B. Anti-PIMT antibody affinity purified on GST-PIMTC matrix was used to detect PIMT protein in HeLa cells. PIMT55 staining (green), DAPI staining of DNA (red), and merged pictures are as indicated.

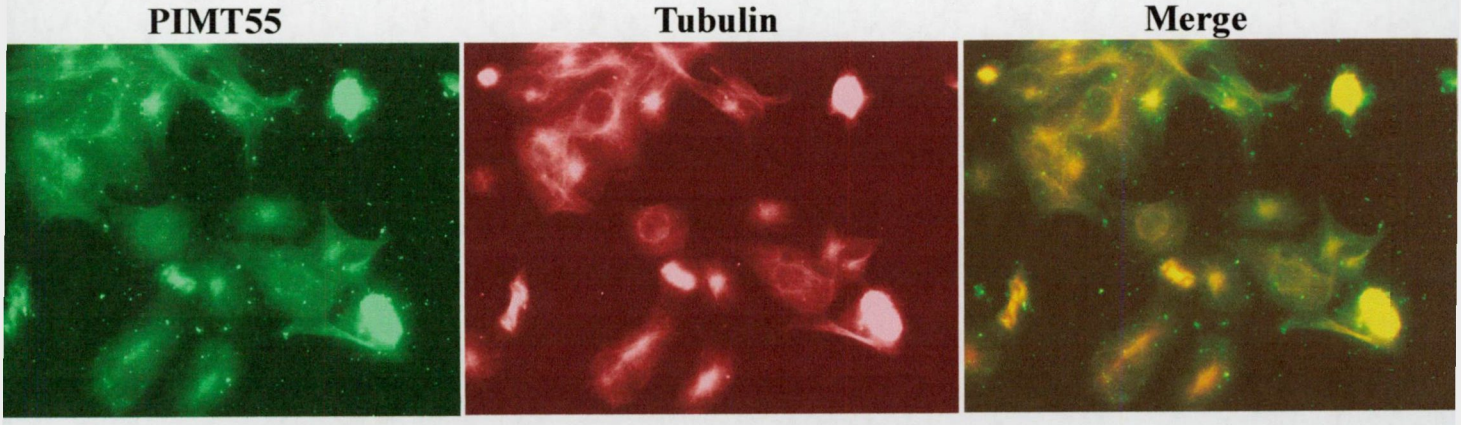

ıre 10A

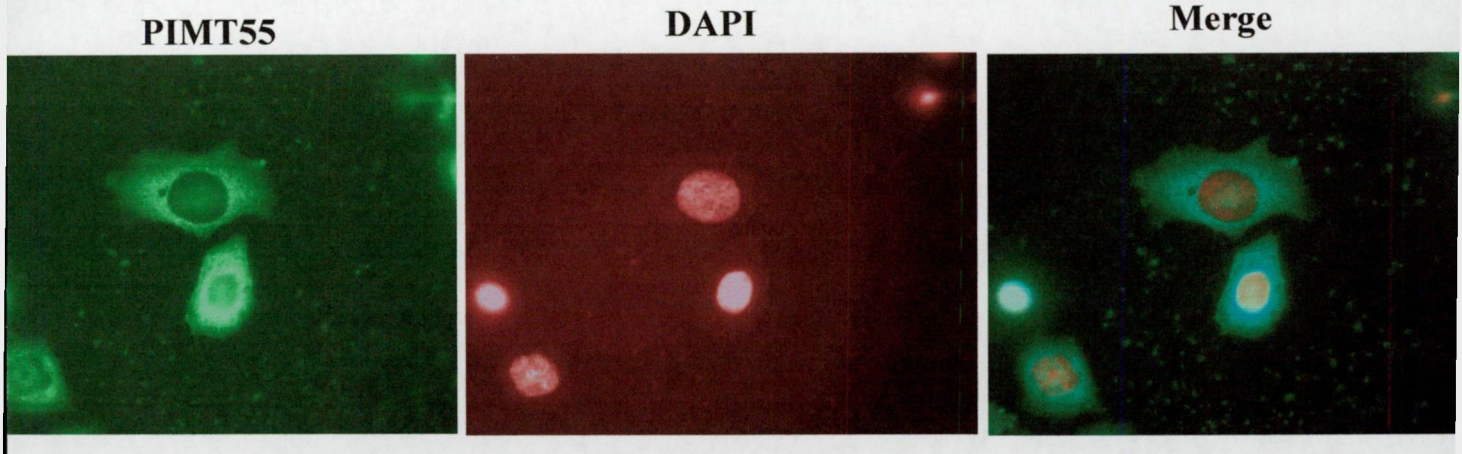

ure 10B

Figure 10. PIMT55 colocalizes with microtubule as its *Drosophila* homologue DTL

A. We made a double localization experiment on HeLa cells, using anti-PIMT55 (green) and anti-tubulin (red) antibodies. In the merged picture the overlapping pattern can be seen as yellow, which is the proof for co-localization of PIMT and microtubules.

B. HeLa cells were treated with microtubule polymerization inhibitor colchicine As a result the cytoskeletal pattern was lost, which indicates that the pattern we observed was really dependent on proper formation of microtubular cytoskeleton.

As expected, double immunolocalization experiments with anti-tubulin and anti-PIMT antibodies showed overlapping patterns (Figure 10A). To further prove that this pattern was identical with the one shown by the microtubule cytoskeleton, cells were treated with the microtubule association inhibitor colchicine for 17 hours before immunolocalization. Addition of colchicine resulted in the diffusion of PIMT55 in the cytoplasm (Figure 10B). From these experiments it was concluded that the 55-kDa isoform of PIMT colocalizes with the microtubule cytoskeleton.

3.2.3. C-terminal region of PIMT interacts with WAIT-1

In order to identify interacting partners of PIMT, a yeast two hybrid screen was carried out using the PIMT-C as a bait against a human hematopoietic cDNA library. Since mouse PIMT and human PIMT have 83% identity and 87% similarity in this region, there were no obstacles to test this type of interaction using a rat homologue agaist a human cDNA library. The strongest interactions were detected with cDNA clones encoding WAIT-1, which was recovered in several independent clones. WAIT-1 is a mammalian homologue of mouse Eed and Drosophila Extra Sex Combs (ESC) proteins (39). Negative controls with unrelated cDNA clones indicated that the PIMT-WAIT-1 interaction was specific (Figure 11).

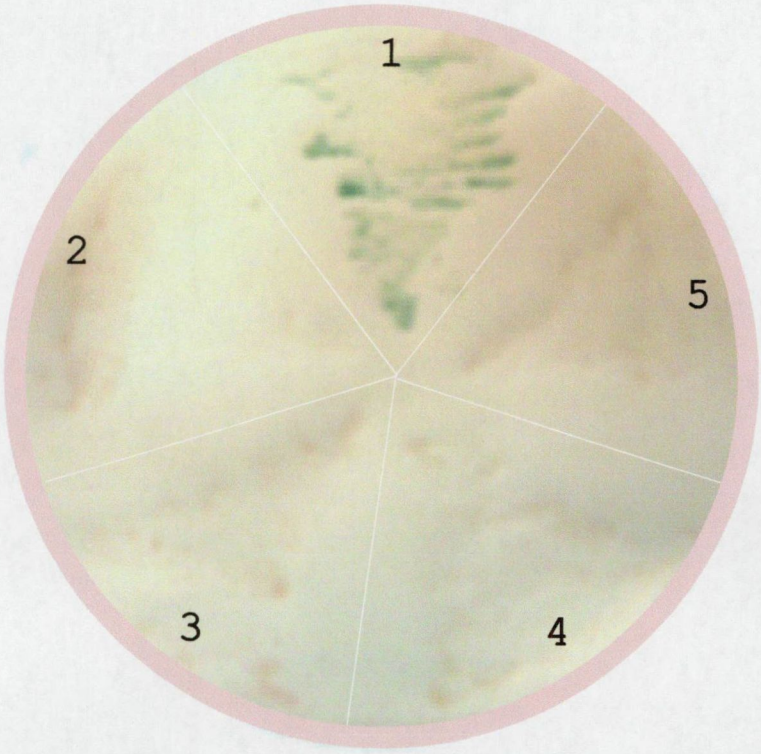

1 PIMT-C/WAIT-1
2 PIMT-C/ADA2B
3 PIMT-C/ADA3(**AAN52142**)
4 ADA2A-1(**AAN88029**) /WAIT-1
5 ADA2B /WAIT-1

Figure 11. The specificity of PIMT and WAIT-1 interaction.

The specificity of the interaction was confirmed by co-transformation of the subject plasmids with unrelated constructs. The colonies were transferred onto nitrocellulose filters and their interaction strength was measured. The beta-galactosidase activities of the unspecific interactions were very weak, while the interaction of the PIMT and WAIT-1 was very strong.

To identify interacting region(s) of WAIT-1 and PIMT, a series of mutations were created in the WAIT-1 and PIMT-C cDNA. The tested WAIT-1 constructs included WAIT1DC, a carboxyl terminal deletion, which removed all WD40 domain; WAIT1DN, an amino terminal deletion that partially removed the 1st WD40 domain, WAIT1DWD2 a deletion that partially removed the 1st and 4th WD40 domains including full removal of 3rd WD40 domain; and WAIT1DWD construct that partially deleted the 5th WD40 domain (Figure 12A).

All mutations generated in WAIT-1 gave negative results in beta-galactosidase assay carried out on agar plates (Figure 12B). These interactions were also quantified in liquid assays (Figure 12A). From these results it was concluded that any mutation disturbing the propeller beta shape of WAIT-1 also abolished its interaction with PIMT. On the other hand, from the experiments with the constructed deletions in PIMT it could be concluded that the WAIT-1 interacting region of PIMT lies within a 91 amino acid long region between amino acids 555-641.

To obtain further experimental support for PIMT-WAIT-1 interaction GST pull-down experiments were carried out. For this WAIT-1 was expressed as a GST fusion protein and mixed with bacterial extract prepared from cells expressing the C-terminal region of PIMT (amino acids 555-852). The resulting complexes were bound to glutathione-sepharose, washed extensively, eluted and analyzed on Western blots. As shown in Figure 13, a significant amount of PIMT was retained on GST-WAIT-1 containing matrixes, while on the controls (matrix alone and GST-bound matrix) no significant amount of PIMT was bound.

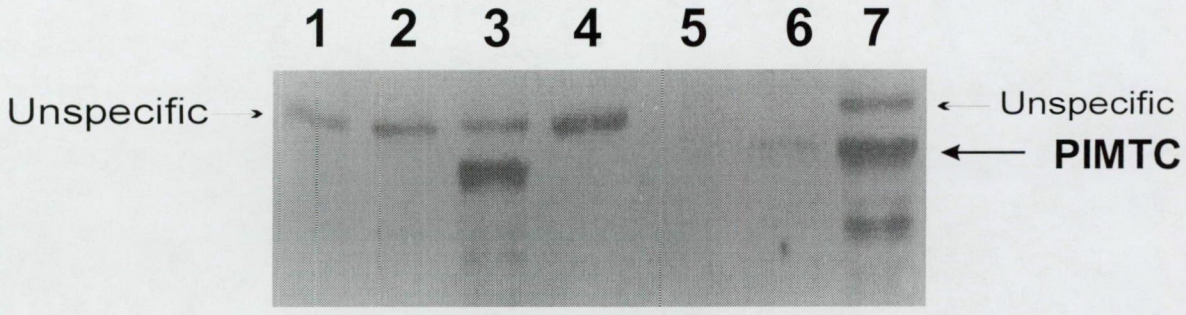

Figure 13. In vitro interaction between GST-WAIT-1 and PIMT.

Western blot developed with PIMT-specific antibody. Lanes 1, 2, and 3 are controls showing bacterial cell extracts used in the pull down experiment: GST (1), GST-WAIT-1 (2), and PIMTC (3). Lanes 4 and 7 contain proteins eluted from GST-WAIT-1 affinity matrix, which was incubated with PBS (4) or with PIMTC (7). Lanes 5 and 6 are controls for nonspecific binding of PIMTC to the matrix showing retention of PIMTC protein on Sepharose beads alone (5), and on GST-Sepharose matrix (6). Arrows show unspecific interaction of PIMTC and bacterial proteins.

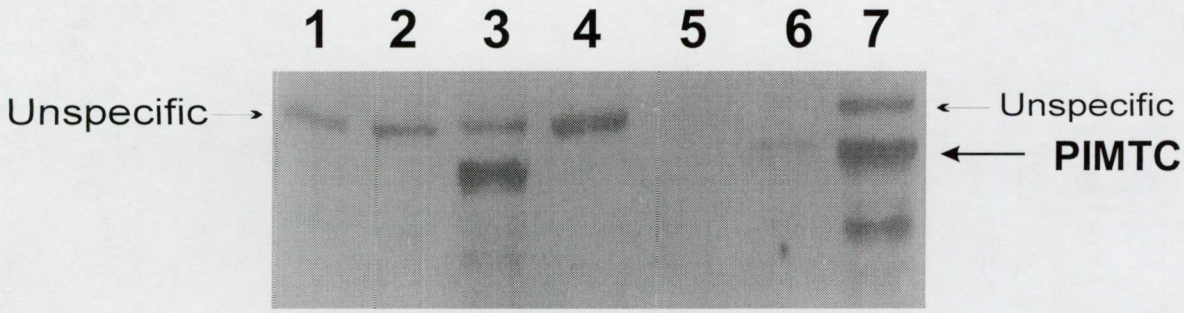

Figure 13. In vitro interaction between GST-WAIT-1 and PIMT.

Western blot developed with PIMT-specific antibody. Lanes 1, 2, and 3 are controls showing bacterial cell extracts used in the pull down experiment: GST (1), GST-WAIT-1 (2), and PIMTC (3). Lanes 4 and 7 contain proteins eluted from GST-WAIT-1 affinity matrix, which was incubated with PBS (4) or with PIMTC (7). Lanes 5 and 6 are controls for nonspecific binding of PIMTC to the matrix showing retention of PIMTC protein on Sepharose beads alone (5), and on GST-Sepharose matrix (6). Arrows show unspecific interaction of PIMTC and bacterial proteins.

Consequently, the GST-pull-down experiment confirmed the observed interaction between WAIT-1 and the C-terminal of PIMT as detected in yeast two hybrid assays.

3.2.4. SiRNA knock down of PIMT in HeLa cells delays cell proliferation

To have more insights about the function of PIMT, PIMT protein was transiently knocked down by using siRNAs specific to PIMT mRNA. siRNAs specific to PIMT and specific to GFP sequences were selected and synthesized according to the criteria and procedure of Donze et al. (36).

Initial experiments were performed to determine the optimum conditions for inducing RNAi with siRNAs in HeLa cells. For this purpose GFP expressing plasmids were co-transfected together with siRNAs specific to GFP. It was found that addition of siRNA specific to GFP specifically reduced the levels of GFP as it was seen from flow cytometer measurements (data not shown) and Western blots (Figure 14). It was concluded that specific RNAi directed to GFP transcript could be induced using our protocol.

For PIMT knock down assay the following controls were used: untreated HeLa cells, unspecific siRNA (siRNA specific to GFP) added, and PIMT specific siRNA added HeLa cells. Western blots of siRNA treated samples showed that PIMT levels specifically decreased (Figure 15A). The DNA was quantified by propidium iodide staining by flowcytometry at 24hrs, 40hrs, and 48hrs after siRNA transfection. The results were analyzed with WinMDI and Cyclhred software.

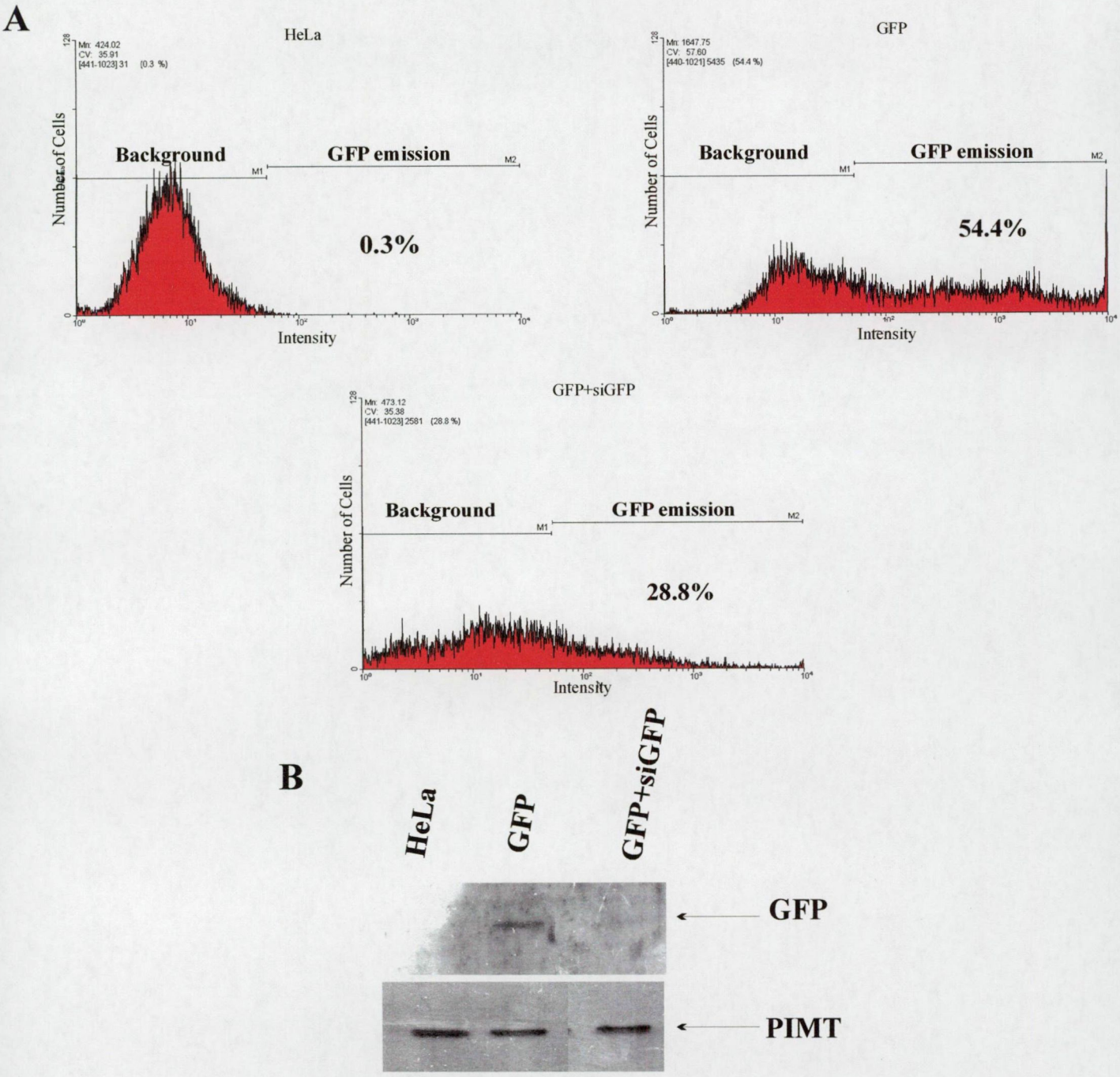

Figure 14. GFP specifically knocked down in HeLa cells

A. SiRNA treated and control samples were analyzed on flow cytometer for their GFP fluorescence. On the graphical representation of data, Y-axis represents number of cells, and X-axis represents the intensity of fluorescence. Cells which have GFP emission are indicated as percentage of total cell population. Samples are: HeLa (absolute control which did not express GFP and was not transfected with GFP specific siRNA); GFP (GFP expressing HeLa cells); GFP+siGFP (GFP expressing and GFP specific siRNA transfected cells).

B. SiRNA treated samples and control samples were blotted and probed with either anti-GFP or anti-PIMT antibodies, and specific bands are indicated with the arrows.

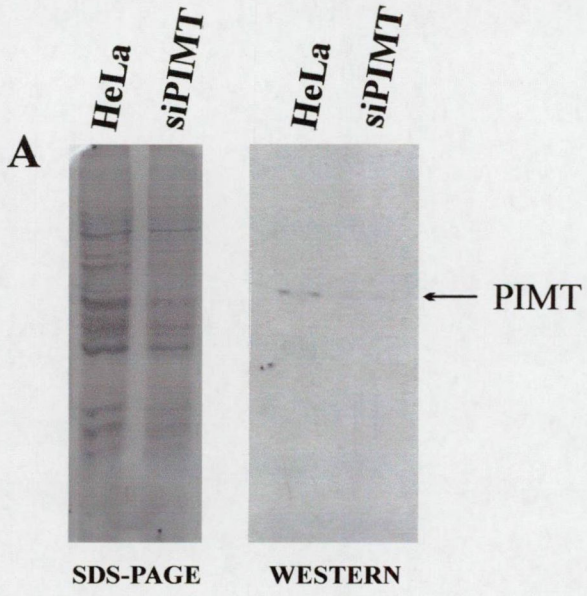

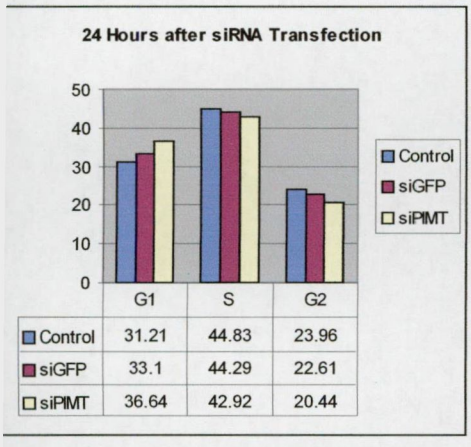

	G1	S	G2
Control	31.21	44.83	23.96
siGFP	33.1	44.29	22.61
siPIMT	36.64	42.92	20.44

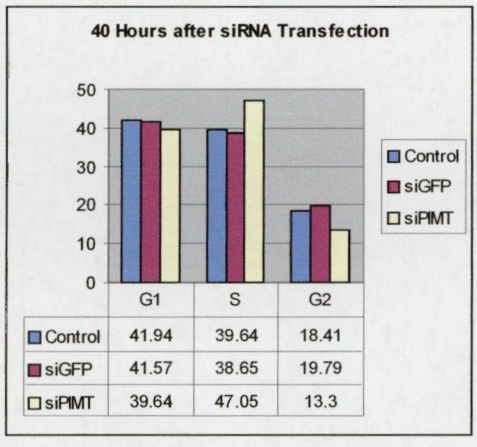

	G1	S	G2
Control	41.94	39.64	18.41
siGFP	41.57	38.65	19.79
siPIMT	39.64	47.05	13.3

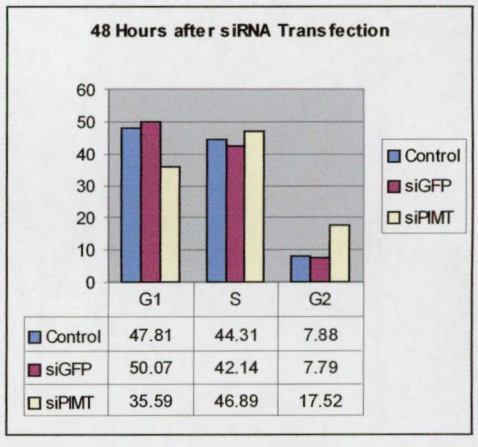

	G1	S	G2
Control	47.81	44.31	7.88
siGFP	50.07	42.14	7.79
siPIMT	35.59	46.89	17.52

Figure 15. Transient knock down of PIMT55 in HeLa cells

To elucidate the function of PIMT55 in HeLa cells, siRNAs against PIMT transcript were synthesized. HeLa cells were transfected with these siRNAs. Two types of control cells were used. Untreated HeLa cells were an absolute control, and the unspecific siRNA treated cells were to check the specificity of RNAi. siRNAs against GFP were used for this purpose.

A. PIMT levels were checked by probing siRNA treated and HeLa controls with anti-PIMT. It was seen that PIMT55 levels specifically decreased in siRNA treated samples.
B. Cells were checked for their DNA content, and analyzed data was represented in this graphic. As it is seen, there was a delay to enter next phase of cell cycle in the siPIMT treated cells in comparison to controls.

This analysis showed that in siRNA treated samples the transition to the next phase of cell cycle was delayed in comparison to the controls. According to the results at 24-hrs the number cells in G1 phase were higher than control. At 40 hrs, S phase cells, and at 48hrs G2/M phase was higher (Figure 15B).

3.2.5. PIMT55 expression increases before S phase

Since the absence of PIMT55 altered cell cycle progressing, it would be that at different stages of cell cycle PIMT55 levels might also change. Although in the previous immunolocalization experiment the level of PIMT expression didn't seem to be changed it is possible that immunolocalization was not sensitive enough in detecting the relative changes in the levels of expression of PIMT55 at different phases of the cell cycle. To check this idea HeLa cells were treated in different ways to arrest the cell cycle at different stages . Cells were serum starved to block in early G1, hydroxyurea treated to block in G1/S phase boundary, and finally colchicine treated to block in G2 phase. Equal amount of protein from each sample was resolved with SDS-PAGE and blotted with PIMT specific antibodies. The results revealed that there was an increase in the PIMT levels in S phase in comparison to other phases (Figure 16).

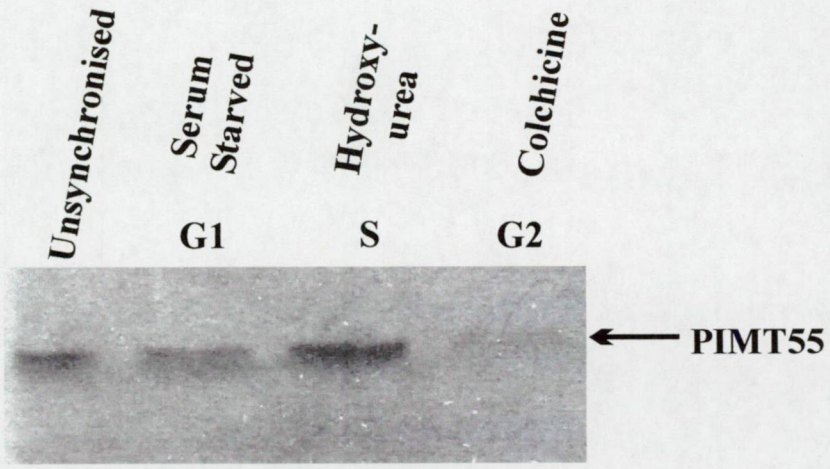

Figure 16. PIMT55 levels at different cell cycle phases

HeLa cells were arrested at different cell cycle phases to determine relative levels of PIMT55 expression. Cells were serum starved to enrich in G0 phase, hydroxyurea treated for G1/S phase boundary, and colchicine treated to arrest at G2. The samples were blotted together with an unsynchronized cell sample. Western blot showed that PIMT55 levels were increased before entering to S

4. DISCUSSION

4.1. DTL is the product of down stream ORF

DTL is encoded by an interesting transcript containing two ORFs. With one base shift towards the 5′-end of the first stop codon the second frame encodes a highly conserved protein among many different species. This structure may code for a single protein by a ribosomal shift during translation. There are examples when both bacterial and eukaryotic ribosomes may perform +1 or –1 frameshifts during translation (37). Since the necessary –1 frameshift could be performed in bacterial system, full length DTL cDNA was cloned and expressed in bacteria. Although in this experiment DTL cDNA was translated in a polycistronic fashion, which is common in bacteria, it showed the possibility that second ORF could be recognized separately by an alternative ribosome binding site.

Therefore, it could be speculated that DTL was translated only from downstream ORF by an internal ribosomal entry site in eukaryotic cell. The specific polyclonal antibodies that were raised against the down stream ORF were affinity purified to improve their specificity and DTL presence was checked in Schneider S2 cells by Western blotting. There were two specific bands recognized by DTLdown antibodies, one with the size of ~60 kDa, and a second with the size of ~120 kDa. However, upstream ORF specific antibodies could not recognize neither of these two bands.

60-kDa protein that we detected in immunoblots, fits to the theoretical molecular weight of a protein translated from the down stream ORF. However, the heavier 120-kDa protein was much heavier than the sum of both ORFs coded by DTL cDNA and was not recognized by DTLup specific antibodies. Therefore, the 60-kDa protein should be a translation product from an internal ribosomal entry site, and the 120-kDa protein is a posttranslational modification of this 60-kDa protein. In the light of these results, the existence of a functional leucine zipper motif

seems to be a relic of evolution. However, antibody specificity for the up stream ORF should be improved for a better understanding judgement of the case.

4.2. Homologues of DTL

Our data base search revealed several homologues of DTL in different species. In the beginning of our investigation, there was not any identified DTL related protein. Mammalian homologues were represented only by EST sequences, which have similarity to the conserved C-terminal of DTL.

Zhu et al. (2001) isolated a nuclear receptor co-activator-interacting protein, designated PIMT, from a human liver cDNA library by using the co-activator peroxisome proliferator-activated receptor-interacting protein (PRIP) as bait in a yeast two-hybrid screen. PIMT (PRIP-interacting protein with methyltransferase domain) cDNA encodes an 852-amino acid protein containing a 9-amino acid methyltransferase motif I (VVDAFCGVG) and an invariant segment (GXXGXXI) found in K-homology motifs of many RNA-binding proteins (38). Northern blot analysis demonstrated ubiquitous expression of a 3.2-kb PIMT transcript, with highest expression in heart, skeletal muscle, kidney, liver, and placenta. It is known that nuclear receptor co-activators participate in the transcriptional activation of specific genes by nuclear receptors (38).

Immunofluorescence studies showed that the 92 kDa PIMT protein and PRIP proteins are colocalized in the nucleus. PIMT binds S-adenosyl-L-methionine, the methyl donor for the methyltransfer reaction, and it also binds RNA, suggesting that it is an RNA methyltransferase (38). Overexpression of PIMT enhances the transcriptional activity of PPARγ and RXR, and this enhancement is further stimulated by overexpression of PRIP, suggesting that PIMT is a component of nuclear receptor signal transduction that acts through PRIP (38).

PIMT has been shown also to interact with a variety of other nuclear receptor co-activators such as CBP, p300, and PBP. PIMT enhanced PBP-mediated transcriptional activity of the PPARγ, as it did for PRIP. On the other hand, PIMT functioned as a repressor of CBP/p300-mediated transactivation of PPARγ (40).

Furthermore in 2002 Mouaikel et. al. identified the yeast homologue of DTL as TGS1p. TGS1p was found to hypermethylate the 5' cap structures of a subset of snoRNAs and localizes to the Cajal bodies in the nucleus as well as in the cytoplasm though the nature of this cytoplasmic localization was not precise (41). Human TGS1 protein (hTGS1), or as it was named earlier PIMT, was also shown to share the same characteristics as the yeast homologue (42). Maturation of most types of RNA requires many complex biochemical reactions, which often occur in an ordered manner that can be described as a processing pathway. RNA maturation can also be associated with a series of specific localizations taken by the RNA (24). In vertebrates snoRNP assembly, 3' end formation and cap tri-methylation are likely to occur in Cajal bodies (19, 41,42).

4.3. Three different isoforms of PIMT exist in different tissues

According to our results from western blots performed on different rat tissues samples, different isoforms PIMT/hTGS1 could be detected. A 55 kDa protein was ubiquitously expressed in all the samples, a 90 kDa protein as described in Zhu et. al. work could be found only in brain and testicular samples, and a 30 kDa protein was only in kidney sample. Furthermore, in HeLa cell line, which was used in the majority of experiments, the 55-kDa isoform was the only detected isoform. However, the sole presence of the 55 kDa isoform can be due to the low levels of the other isoforms, which may be exceeding the sensitivity of western blot analysis. Therefore,

55kDa isoform being the most commonly expressed product, was easily detected in the samples examined.

PIMT gene contains more than 13 exons according to Zhu et. al. (38). This suggests that alternatively spliced variations of PIMT mRNA may result in different isoforms of PIMT protein. The presence of shorter cDNA sequences related to PIMT in database also supports the idea that the alternatively spliced versions of *PIMT/hTGS1* gene exist.

4.4. DTL and 55-kDa isoform of PIMT are cytoplasmic, microtubule cytoskeleton associated proteins

Western blots of cytoplasmic and nuclear fractions of insect and mammalian cell lines showed that DTL and PIMT55, the 55-kDa isoform of PIMT localize in the cytoplasm. Immunolocalization experiments added to this fact the coexistence of DTL and PIMT together with microtubule cytoskeleton. In the light of our results, we can speculate that the nuclear localization of PIMT/hTGS1 may be restricted to the 90-kDa isoform, while 55-kDa isoform is a cytoplasmic protein. However it is obvious that a major property of this family that is the cytoskelatal localization, was omitted in the publications mentioned above.

4.5. Human DTL interacts with WAIT-1

BLAST searches and amino acid sequence multi-alignments showed that DTL related proteins are highly conserved through their C-terminal end. Therefore, we focused our attention to this region for further analyses. We performed a yeast two-hybrid screen using C-terminal of PIMT/hTGS1 as bait against a human hematopoietic cDNA library. This screen demonstrated the interaction between PIMT/hTGS1 and WAIT-1 (NP_003788) proteins. Using deleted versions of the bait/prey constructs or non-specific constructs further supported this interaction. With GST pull down assays we proved the interaction between human DTL and WAIT-1 proteins *in vitro*.

WAIT-1 is a mammalian homologue of mouse Eed (Embryonic Ectoderm Development) and *Drosophila* ESC (Extra Sex Combs) proteins (39). These two proteins belong to the polycomb group of proteins, that act by altering the accessibility of DNA to factors required for gene transcription (43).

In mice, the PcG protein Eed is present in a distinct complex that interacts with histone deacetylase (HDAC) and the PcG member Ezh2 (Enhancer of zeste homolog 2) (43). Recent findings showed that histone (H3-K27) methylation colocalizes with, and is dependent on binding of an EED-EZH2 complex to an Ultrabithorax (Ubx) Polycomb response element (PRE).

On the other hand WAIT-1 specifically interacts with the cytoplasmic domains of integrin β7, α4, and αE subunits localizing to very different compartments than its homologues (39). That shows that human EED by itself may localize to nucleus, but certain isoforms of EED may be restricted to cytoplasm.

The β–subunits of integrins are considered important for regulation of stimulated cell adhesion and adhesion-dependent signal transduction (45). The cytoplasmic tails of the β7 subunit are critical for integrin function because they regulate receptor avidity and signaling (45). It may be that WAIT-1 shuttles between membrane-associated β7-integrins and the nucleus, thereby linking cell adhesion and signal transduction or it is involved in regulation of gene expression (39).

WAIT-1 is a WD40 repeat protein. WD or WD40 domain, are found in a number of eukaryotic proteins that cover a wide variety of functions including adaptor/regulatory modules in signal transduction, pre-mRNA processing and cytoskeleton assembly (46). The consensus sequence typically contains a GH dipeptide 11-24 residue from its N-terminus and the WD dipeptide at its C-terminus and is 40 residues long. This gives the name WD40 to the domain

(46). WD40 repeats create a closed ring propeller-structure, which is a platform for proteins to bind either stably or reversibly (46). Residues on the top and bottom surface of the propeller are proposed to coordinate interactions with other proteins and/or small ligands (46).

4.6 Function of DTL

siRNA knock down of PIMT55 in HeLa cells revealed that absence of PIMT55 interfered with cell cycle progression. Moreover, protein samples enriched in different cell cycle stages showed that PIMT55 levels increase in S phase. This observation is another proof of the relation between PIMT55 and cell cycle. Previously it was shown that knock down of *C. elegans* homologue of PIMT (T08G11.4) resulted in abnormal spindle orientation, slow growth and larval lethality (47).

There are eukaryotic proteins that have been identified as splicing factors and independently as essential for cell cycle progression (48). Previously it was shown that in yeast, tubulin pre-mRNA splicing and cell cycle control is linked to each other (49,50).

Therefore delayed cell cycle progression can be explained by the fact that reduction of the PIMT/hTGS1 levels should also reduce the rate of sn(o)RNA maturation, and this in its turn should disable the proper splicing of mRNAs and editing of rRNA.

However, abnormal spindle orientation that is observed in C. elegans, can be indicator of a more elaborate function of PIMT/hTGS1 than just efficient splicing of mRNAs (including tubulin mRNA) or ribosomal RNA maturation. PIMT55 colocalization with microtubules and its interaction with WAIT-1 suggest a potential pathway for signals from cell-cell contact and cell-matrix interaction to influence cytoskeletal structure in higher eukaryotes. There is evidence that spindle orientation correction is related with cortex interactions (namely with actin structures) of the very short astral microtubules (51). Probably, through astral microtubule-mediated delivery of a signal from the periphery i.e. integrin or actin cytoskeleton, has a role on this function.

On the other hand evidence suggests that the bulk of the mRNAs in the cytoplasm, are cytoskeleton-bound (52). This indicates that there are probably a number of so-called "general" RNA-binding proteins within eukaryotic cells that mediate the interaction between a broad range of mRNAs and the cytoskeleton. 55-kDa version of PIMT/hTGS1 may be one of these general RNA-binding cytoskeleton-associated proteins. Its uniform distribution throughout of microtubule cytoskleton rather supports this possibility.

5. CONCLUSIONS

- DTL is translated as a 60 kDa protein from an internal ribosomal entry site in *Drosophila* Schneider S2 cells. DTL has also a higher molecular weight isoform which is 120 kDa and probably is the result of a post-translationally modified version of 60 kDa isoform.
- Both isoforms of DTL are cytoplasmic proteins and are colocalized with microtubule cytoskeleton.
- Mammalian homologue of DTL has three isoforms: 90 kDa isofrom is translated in brain and heart tissues in mouse; 55 kDa isoform is ubiquitously translated in all tissues examined; 30 kDa isoform is only found in kidney tissue samples.
- In human HeLa cells 55 kDa isoform of the mammalian DTL is the major product. 55 kDa protein is a cytoplasmic protein and colocolizes with microtubule cytoskeleton as DTL.
- Mammalian DTL interacts with WAIT-1 protein through its carboxyl-terminal.
- SiRNA inhibition of mammalian DTL interferes with proper cell cycle progression in HeLa cells.

6. SUMMARY

RNA-protein interactions direct a diverse variety of cellular processes, which range from transcriptional regulation to targeted translation of proteins. Hence, to discover new proteins with a specific affinity to RNA molecules and find out their specific function will expand our understanding on a wide range of cellular functions. Following this statement, a screen was developed to search *Drosophila* proteome for RNA binding proteins and an unknown protein with RNA binding property was retrieved (Udvardy et al.). Since in the screen, TAR (Transactivation Response RNA element) RNA of HIV was used as a bait the cDNA fragment representing a so far unknown gene designated as *dtl* (Drosophila Tat Like) gene was isolated. In this work we aimed to characterize this new *Drosophila* protein and its mammalian homologue.

The retrieved protein had well conserved homologues in different species and is represented with many ESTs (expressed sequence tags) in databases suggesting an important role in cellular function. In the beginning of our work none of the homologues had an identified function. However during our investigation, other research groups revealed certain aspects of the functional properties of this new class of proteins.

To identify functional domains through conserved domains of homologous proteins, database search was performed. This search revealed that DTLdown had several homologues in different species extending from yeast to human. The most conserved motifs found in similar methylase domains were a 9-amino acids methyltransferase Motif I (VVDAFCGVG), a 7-amino acids Motif II (KADVVFL), and an S-adenosyl-L-methionine interacting region.

Our other conclusions about the work are:

- In *Drosophila* Schneider S2 cells two isoforms of DTL exists. 60 kDa isoform is translated from an internal ribosomal entry site, and 120 kDa protein is a post-translational modified

version of the 60 kDa protein. Both isoforms of DTL are cytoplasmic proteins and are colocalized with microtubule cytoskeleton.

- Mammalian homologue of DTL has three isoforms translated in rat tissues: 90 kDa isofrom is translated in brain and heart tissues; 55 kDa isoform is ubiquitously translated in all tissues examined; 30 kDa isoform is only found in kidney tissue samples.
- 55 kDa isoform of the mammalian DTL is the major product in human HeLa cells. 55 kDa protein is a cytoplasmic protein and colocolizes with microtubule cytoskeleton as DTL.
- Mammalian DTL interacts with WAIT-1 protein through its carboxyl-terminal. β-propellar structure of WAIT-1 formed by the WD repeats is essential for this interaction.
- SiRNA inhibition of mammalian DTL interferes with proper cell cycle progression in HeLa cells.

7. ÖSSZEFOGLALÓ

RNS-fehérje kölcsönhatások számos sejtszintű folyamatban vesznek részt, a transzkripció szabályozástól a fehérjék kifejeződéséig. Sokrétű szerepük révén új RNS-kötő fehérjék azonosítása hozzájárulhat a sejtekben lejátszódó folyamatok alaposabb megértéséhez. Ezen gondolat mentén RNS-kötő fehérjéket *kerestünk Drosophila melanogaster*ben, és egy addig még funkcionálisan nem ismert géntermékét azonosítottunk (Udvardy és mtsai). Mivel a screen-ben a HIV vírus TAR RNS-ét használtuk, az így azonosított fehérjét DTL-nek (*Drosophila* TAT Like) neveztük el. Ebben a munkában célul tűztük ki az ecetmuslica fehérje és emlős homológjának karakterizálását.

A DTL fehérje homológjai számos más organizmusban is fellelhetők, az adatbázisokban több EST is reprezentálja, ami arra utal, hogy fontos szerepet játszhat a sejt életében. A munkánk kezdetekor egyik DTL homológnak sem azonosították a funkcióját, bár kutatásaink közben más csoportok leírták bizonyos tulajdonságait ennek az új fehérje családnak.

A fehérje funkcionális doménjeinek azonosítása érdekében adatbázisokban szekvencia összehasonlításokat végeztünk. Szekvencia hasonlóságok alapján több homológ fehérjét azonosítottunk számos organizmusban, az élesztőtől az emberig. Három erősen konzervált régiót azonosítottunk: a kilenc aminosavból álló metiltranszferáz motívum I-et (VVDAFCGVG), a hét aminosavas metiltranszferáz motívum II-őt (KADVVFL) és egy S-adenozil-L-metionin kötő régiót.

A munkánk további konklúziói:

- *Drosophila melanogaster* Schneider S2 sejtekben két DTL izoforma létezik. Egy 60 kDa-os fehérje belső transzlációs startpontról képződik, míg egy 120 kDa-os változat

posztranszlációs modifikáció következtében keletkezik. Mindkét DTL izoforma a citoplazmában helyezkedik el, és a mikrotubulusokhoz asszociálódik.

- DTL emlős homológjának három izoformája létezik patkány szövetekben: a 90 kDa izoforma agy és szív preparátumokban fejeződik ki, 55 kDa-os izoforma minden vizsgált szövetben jelen volt, és egy 30 kDa-os izoforma kizárólag veséből származó mintákban volt detektálható.
- Az emlős DTL 55 kDa-os változata az abundáns izoforma humán HeLa sejtekben. Ez a fehérje a citoplazmában található, és mint a DTL, a citoszkeletonhoz kapcsolódik.
- Az emlős DTL a C-terminális részén keresztül kölcsönhatásba lép a WAIT-1 fehérjével. A WAIT-1 β-propeller struktúrája, amit WD ismétlések alkotnak, esszenciális a DTL-lel való kölcsönhatáshoz.
- Az emlős DTL siRNS-ekkel való gátlása zavarja a normális sejtciklust HeLa sejtekben.

8. REFERENCES

1. Shen LX, Cai Z, Tinoco I Jr. (1995) RNA structure at high resolution. *FASEB J* **9**(11):1023-33
2. Tinoco I Jr, Bustamante C. (1999) How RNA folds. *J Mol Biol.* 293(2):271-81.
3. Crowder S, Holton J, Alber T. (2001) Covariance analysis of RNA recognition motifs identifies functionally linked amino acids. *J Mol Biol.* **310(4)**:793-800.
4. Braddock DT, Louis JM, Baber JL, Levens D, Clore GM. (2002) Structure and dynamics of KH domains from FBP bound to single-stranded DNA. *Nature* **415**: 1051 - 1056
5. Saunders LR, Barber GN. (2003) The dsRNA binding protein family: critical roles, diverse cellular functions. *FASEB J* **17(9)**:961-83.
6. Laity JH, Lee BM, Wright PE. (2001) Zinc finger proteins: new insights into structural and functional diversity. *Curr Opin Struct Biol* **11(1)**:39-46.
7. Smith CA, Calabro V, Frankel AD. (2000) An RNA-binding chameleon. *Mol Cell.* **6(5)**:1067-76.
8. Williamson JR. (2000) Induced fit in RNA-protein recognition. *Nat Struct Biol* **7(10):**834-7
9. Karn J. (1999) Tackling Tat. *J Mol Biol* **293(2):**235-54
10. Stulke J. (2002) Control of transcription termination in bacteria by RNA-binding proteins that modulate RNA structures. *Arch Microbiol.* **177(6):**433-40.
11. Wayne A. Decatur and Maurille J. Fournier (2003) RNA-guided Nucleotide Modification of Ribosomal and Other RNAs *J Biol Chem.* **278(2):**695-8.
12. Collins K. (2000) Mammalian telomeres and telomerase. *Curr Opin Cell Biol.* **12(3):**378-83.
13. Will CL, Luhrmann R. (2001) Spliceosomal UsnRNP biogenesis, structure and function. Curr Opin Cell Biol. **13(3):**290-301

14. Reed R, Magni K. (2001) A new view of mRNA export: separating the wheat from the chaff. *Nat Cell Biol.* **3(9):**E201-4

15. Dreyfuss G, Kim VN, Kataoka N. (2002) Messenger-RNA-binding proteins and the messages they carry. *Nat Rev Mol Cell Biol.* **3(3):**195-205.

16. Jansen RP. (1999) RNA-cytoskeletal associations. *FASEB J* **13(3):**455-66

17. Dean KA, Aggarwal AK, Wharton RP. (2002) Translational repressors in Drosophila. Trends Genet. 11 572-7.

18. Guhaniyogi J, Brewer G. Regulation of mRNA stability in mammalian cells. (2001) *Gene* **265:**11-23

19. Decatur WA, Fournier MJ (2003) RNA-guided nucleotide modification of ribosomal and other RNAs. *J Biol Chem* **278(2):**695-8

20. Weinstein LB, Steitz JA. Guided tours: from precursor snoRNA to functional snoRNP (1999) *Curr Opin Cell Biol.* **11(3):**378-84.

21. Kiss T. (2001) Small nucleolar RNA-guided post-transcriptional modification of cellular RNAs.*EMBO J.* **20(14):**3617-22.

22. Maas S, Rich A. (2000) Changing genetic information through RNA editing. *Bioessays.* **22(9)**:790-802.

23. Grams J, McManus MT, Hajduk SL. (2000) Processing of polycistronic guide RNAs is associated with RNA editing complexes in Trypanosoma brucei. *EMBO J.* **19(20):**5525-32.

24. Kiss T. (2002) Small nucleolar RNAs: an abundant group of noncoding RNAs with diverse cellular functions. *Cell* **109(2):**145-8.

25. Dreyfuss G, Kim VN, Kataoka N. (2002) Messenger-RNA-binding proteins and the messages they carry. *Nat Rev Mol Cell Biol.* **3(3):**195-205

26. Collins CA, Guthrie C. (2000) The question remains: is the spliceosome a ribozyme? *Nat Struct Biol.* **7(10):**850-4.

27. Akker SA, Smith PJ, Chew SL. (2001) Nuclear post-transcriptional control of gene expression. *J Mol Endocrinol* **27(2):**123-31

28. . Norton PA. (1994) Alternative pre-mRNA splicing: factors involved in splice site selection. *J Cell Sci.* **107:**1-7.

29. Garcia-Martinez LF, Mavankal G, Peters P, Wu-Baer F, Gaynor RB. (1995) Tat functions to stimulate the elongation properties of transcription complexes paused by the duplicated TAR RNA element of human immunodeficiency virus 2. J Mol Biol. 254(3):350-63.

30. . Campisi DM, Calabro V, Frankel AD.(2001) Structure-based design of a dimeric RNA-peptide complex. *EMBO J.* **20(1-2):**178-86

31. Vendel AC, Lumb KJ.. (2003). Molecular recognition of the human coactivator CBP by the HIV-1 transcriptional activator Tat. *Biochemistry* **42(4):**910-6

32. . Marzio G, Tyagi M, Gutierrez MI, Giacca M. (1998) HIV-1 tat transactivator recruits p300 and CREB-binding protein histone acetyltransferases to the viral promoter. *Proc Natl Acad Sci U S A.* **95(23)**:13519-24.

33. Ott M, Schnolzer M, Garnica J, Fischle W, Emiliani S, Rackwitz HR, Verdin E. (1999) Acetylation of the HIV-1 Tat protein by p300 is important for its transcriptional activity. *Curr Biol* **9(24):**1489-92.

34. Chen D, Wang M, Zhou S, Zhou Q. (2002) HIV-1 Tat targets microtubules to induce apoptosis, a process promoted by the pro-apoptotic Bcl-2 relative Bim. *EMBO J.* **21(24):**6801-10.

35. Sambrook J, Fritsch EF, Maniatis T. (1989) Molecular cloning . A laboratory manual. *Cold Spring Harbor Laboratory Press.*

36. Donze O, Picard D. (2002) RNA interference in mammalian cells using siRNAs synthesized with T7 RNA polymerase. *Nucleic Acids Res.* **30(10):**e46.

37. Horsfield JA, Wilson DN, Mannering SA, Adamski FM, Tate WP. (1995) Prokaryotic ribosomes recode the HIV-1 gag-pol-1 frameshift sequence by an E/P site post-translocation simultaneous slippage mechanism. *Nucleic Acids Res.* **23(9):**1487-94

38. Zhu Y, Qi C, Cao WQ, Yeldandi AV, Rao MS, Reddy JK. (2001) Cloning and characterization of PIMT, a protein with a methyltransferase domain, which interacts with and enhances nuclear receptor coactivator PRIP function. *Proc Natl Acad Sci U S A.* **98(18):**10380-5.

39. Rietzler M, Bittner M, Kolanus W, Schuster A, Holzmann B. (1998) The human WD repeat protein WAIT-1 specifically interacts with the cytoplasmic tails of beta7-integrins. *J Biol Chem. Oct* **273(42):**27459-66

40. Misra P, Qi C, Yu S, Shah SH, Cao WQ, Rao MS, Thimmapaya B, Zhu Y, Reddy JK. (2002) Interaction of PIMT with transcriptional coactivators CBP, p300, and PBP differential role in transcriptional regulation. *J Biol Chem.* **277(22):**20011-9

41. Mouaikel J, Verheggen C, Bertrand E, Tazi J, Bordonne R. (2002) Hypermethylation of the cap structure of both yeast snRNAs and snoRNAs requires a conserved methyltransferase that is localized to the nucleolus. *Mol Cell.* **9(4):**891-901.

42. Verheggen C, Lafontaine DL, Samarsky D, Mouaikel J, Blanchard JM, Bordonne R, Bertrand E. (2002) Mammalian and yeast U3 snoRNPs are matured in specific and related nuclear compartments. *EMBO J.* **21(11):**2736-45.

43. Orlando V. (2003) Polycomb, epigenomes, and control of cell identity. *Cell.* **112(5):**599-606.

44. Cao R, Wang L, Wang H, Xia L, Erdjument-Bromage H, Tempst P, Jones RS, Zhang Y. (2002) Role of histone H3 lysine 27 methylation in Polycomb-group silencing. *Science.* **298(5595):**1039-43.

45. .Hynes RO. (2002) Integrins: bidirectional, allosteric signaling machines.*Cell.* **110(6):**673-87.

46. Li D, Roberts R. (2001) WD-repeat proteins: structure characteristics, biological function, and their involvement in human diseases. *Cell Mol Life Sci.* **58(14):**2085-97.

47. Zipperlen P, Fraser AG, Kamath RS, Martinez-Campos M, Ahringer J. (2001) Roles for 147 embryonic lethal genes on C.elegans chromosome I identified by RNA interference and video microscopy. *EMBO J.* **20(15):**3984-92

48. Dahan O, Kupiec M. (2002) Mutations in genes of Saccharomyces cerevisiae encoding pre-mRNA splicing factors cause cell cycle arrest through activation of the spindle checkpoint. *Nucleic Acids Res.* **30(20):**4361-70.

49. . Burns CG, Ohi R, Mehta S, O'Toole ET, Winey M, Clark TA, Sugnet CW, Ares M Jr, Gould KL (2002) Removal of a single alpha-tubulin gene intron suppresses cell cycle arrest phenotypes of splicing factor mutations in Saccharomyces cerevisiae.*Mol Cell Biol.* **22(3):**801-15.

50. Chawla G, Sapra AK, Surana U, Vijayraghavan U. (2003) Dependence of pre-mRNA introns on PRP17, a non-essential splicing factor: implications for efficient progression through cell cycle transitions. *Nucleic Acids Res.* 31(9):2333-43.

51. Hwang E, Kusch J, Barral Y, Huffaker TC. (2003) Spindle orientation in Saccharomyces cerevisiae depends on the transport of microtubule ends along polarized actin cables. *J Cell Biol.* **161(3):**483-8.

52. Jansen RP. (1999) RNA-cytoskeletal associations. *FASEB J.* **13(3):** 455-66.

Acknowledgement

I would like to thank to the following people and institutions for their support that allowed me to accomplish this thesis.

To Prof. Boros Imre for giving me the chance to work in his group, for his guidance and support.

To Prof. Udvardi Andor for his helps and advises.

To Dr. Selen Muratoğlu, Ökrös Katalin and Pápai Gábor for their collaborations and their great friendship.

To my parents Gülkend and Nejat Enünlü, my aunt Mina Baykara, and my beloved wife Natalya Enünlü for their continuous support and affection.

To all the friends from ITC and BRC community for their cheerful existence.

This project was sponsored from grants of the Hungarian Science Fund (OTKA T29939) and Hungarian Ministry of Education (FKFP 0060/2000) and accomplished in the laboratories of Biological Research Center of Hungarian Academy of Sciences under the supervision of Prof. Boros Imre.

I would also like to acknowledge that TUBITAK (Turkish Scientific and Technical Research Institution) financed 4 years of my stay in Hungary during my PhD work.